SHORT COMMUNICATION

Endogenous ZAP is associated with altered global cellular gene expression during Zika virus infection

Nguyen Phuong Khanh Le[1], Prince Pal Singh[1,2], Ahmad Jawad Sabir[3], Ivan Trus[4], Uladzimir Karniychuk[1,*]

[1]Department of Veterinary Biosciences, College of Veterinary Medicine, The Ohio State University, Columbus, OH, USA

[2]School of Public Health, University of Saskatchewan, Saskatoon, Canada

[3]Department of Microbiology and Immunology, University of Illinois, College of Medicine, Chicago, IL, USA

[4]Dioscuri Centre for RNA-Protein Interactions in Human Health and Disease, International Institute of Molecular and Cell Biology, Warsaw, Poland

*** Correspondence:** Uladzimir Karniychuk

Department of Veterinary Biosciences, College of Veterinary Medicine, The Ohio State University, Columbus, OH, USA

karniychuk.1@osu.edu

Abstract

The zinc finger antiviral protein 1 (ZAP) has broad antiviral activity. Previous RNA-seq analyses were conducted in uninfected wild-type and ZAP-KO cells; however, the impact of ZAP on global gene expression during virus infection remains unknown. Here, we characterized global cellular gene expression in uninfected and Zika virus-infected wild-type and ZAP knockout VERO cells. ZAP is an interferon (IFN)-stimulated gene, which itself may enhance type I IFN antiviral response. We found that ZAP was associated with the inhibition of Zika virus in the absence of a robust type I IFN system (VERO cells are deficient for IFN-alpha and -beta). Also, during Zika infection in VERO cells endogenous ZAP was associated with amplification of global transcriptional antiviral responses in the absence of a robust type I IFN system. Further studies are warranted to elucidate this type I IFN-independent antiviral activity directly or indirectly mediated by ZAP.

Keywords: **Flavivirus, Zika virus, Zinc finger antiviral protein, ZAP, interferon, RNA-seq**

47 **INTRODUCTION**

48 The zinc finger CCCH-type antiviral protein 1 (ZAP) is a cellular protein with broad antiviral
49 activity [1-5]. ZAP binds viral RNA mediating degradation and translational inhibition [3].
50 While ZAP lacks intrinsic RNase activity, it recruits the 5′ and 3′ RNA degradation machinery
51 [6,7]. Using a murine leukemia reporter virus, DDX17 and DHX30 cellular RNA helicases were
52 identified as ZAP co-factors [8,9]. The E3 ubiquitin ligase TRIM25 enhances ZAP activity
53 against alphaviruses [10,11]. ZAP also interacts with the cytoplasmic protein KHNYN to inhibit
54 CpG-enriched human immunodeficiency virus 1 (HIV-1) [12]. Recently, Riplet, a protein known
55 for activating the retinoic acid-inducible gene I, was identified as a ZAP co-factor [13]. Initially
56 characterized to inhibit murine leukemia virus [14], ZAP has shown efficacy against many
57 viruses, including alphaviruses, filoviruses, influenza virus, porcine reproductive and respiratory
58 syndrome virus, hepatitis B virus, human cytomegalovirus, human T-cell lymphotropic virus
59 type 1, and HIV-1 [1,15-24]. However, ZAP's antiviral efficiency is limited against certain
60 RNA viruses, including vesicular stomatitis virus, poliovirus, enterovirus A71, herpes simplex
61 virus type 1, and some flaviviruses [7,15,25]. Emerging flaviviruses constantly threaten public
62 health. A previous study showed the sensitivity of Japanese encephalitis virus (JEV) to
63 overexpressed ectopic and endogenous ZAP [7]. In contrast, yellow fever virus (YFV), dengue
64 virus (DENV), and Zika virus were categorized as ZAP-resistant [7,15]. Zika virus sensitivity
65 was tested by ectopically overexpressing ZAP against the background of endogenous ZAP.
66 Overexpression screening is a powerful approach, but overexpressing individual genes may also
67 miss antiviral effectors that work in multiprotein complexes [26]. Here, we compared Zika virus
68 infection and characterized global cellular gene expression in uninfected and Zika-infected wild-
69 type and ZAP knockout VERO cells.

MATERIALS AND METHODS

Cells

We maintained wild-type VERO E6 cells (ATCC; VERO-ZAP-WT) and ZAP knockout (ZAP-KO) derivatives (VERO-ZAP-KO) in DMEM (Fisher; # 11-965-118) supplemented with 10% heat-inactivated fetal bovine serum (FBS, Fisher; #A5256801), 1x Penicillin-Streptomycin (Fisher; #15140122), and 2.67 mM sodium bicarbonate (Fisher; # 25080094) at +37°C in a 5% CO_2 humidified incubator. To generate ZAP-KO cell line, we used the guide RNA (gRNA) GTCTCTGGCAGTACTTGCGA which targets the first exon of *Chlorocebus sabaeus* (Gene ID: 103226990) ZC3HAV1 gene, which is required for the expression of all ZAP isoforms. We also used a non-targeting control gRNA ACGGAGGCTAAGCGTCGCAA for control cells. These gRNAs were transiently transfected into cells using GenCrispr NLS-Cas9-NLS Nuclease (GenScript). Subsequently, transfected cells were seeded in 96-well plates through limiting dilution to generate isogenic single clones. Following expansion, the clones were genotyped via Sanger sequencing, employing primers (ATCGCTGGGCTGGACTAACG, GCAGAGAAGGGAGTGGCTGAA) to identify indels. The knockout subclone verified by genotyping was further confirmed by western blot for ZAP expression (**Fig 1A**) as described below. The negative control cells were not isolated into single clones, but they were validated by Sanger sequencing to confirm there were no indels. We confirmed the absence of mycoplasma contamination in cells using the LookOut Mycoplasma PCR Detection Kit (Millipore Sigma).

Viruses

We utilized the Asian lineage Zika virus H/PF/2013 strain [GenBank: KJ776791.2]. Zika virus was synthetically rescued using reverse genetics following previously described methods [27].

93 Subsequently, the virus was propagated in VERO cells cultured in DMEM supplemented with
94 2% FBS and 1% penicillin/streptomycin (P/S). Supernatants were harvested, centrifuged (12,000
95 g, 20 min, +4°C), aliquoted, and frozen (-80°C). Infectious virus titers were quantified using
96 VERO cells via and endpoint dilution assay. The fifty percent tissue culture infective dose
97 ($TCID_{50}$) endpoint titers were calculated as previously described [27-30]. Media from virus-
98 negative VERO cells was processed in the same manner as the virus stocks and used as control.
99 The absence of mycoplasma contamination in the virus stocks was confirmed using the LookOut
100 Mycoplasma PCR Detection Kit (Millipore Sigma; #MP0035).
101

102 **Comparative RNA-seq analysis in wild-type and ZAP-KO cells**

103 VERO-ZAP-WT and VERO-ZAP-KO cells were seeded at 6×10^5 cells per well in 6-well plates,
104 with 4 plates per cell line, in DMEM supplemented with 10% FBS for 24 h. Wells in two plates
105 from each cell line were either mock-inoculated with media from virus-negative cells (4-6 well
106 replicates for VERO-ZAP-WT and VERO-ZAP-KO) or inoculated with MOI 1 of Zika virus (6
107 well replicates for VERO-ZAP-WT and VERO-ZAP-KO). After 2 h at 37ºC, the inoculum was
108 removed, cells were washed, and covered with DMEM supplemented with 2% FBS, then
109 maintained at 37ºC. At 24 h and 72 h post-inoculation, media was removed, cells were washed
110 with commercial 1× PBS, homogenized in 1 mL of TRI Reagent Solution (Fisher; # AM9738),
111 and RNA was extracted according to the manufacturer's protocol using the PureLink RNA Mini
112 Kit (Fisher; 12-183-018A). A total of 4-6 replicate samples were obtained for mock-inoculated
113 VERO-ZAP-WT, mock-inoculated VERO-ZAP-KO, Zika-infected VERO-ZAP-WT, and Zika-
114 infected VERO-ZAP-KO cells, at both 24 and 72 h. RNA quantification was performed using the
115 Qubit RNA High Sensitivity kit (Fisher; # Q32855) and Qubit 2.0 Fluorometer (Fisher). RNA

116 quality was assessed using a bioanalyzer (Agilent Technologies 2100) to ensure all samples had
117 RNA Integrity Number (RIN) values above 9.0. DNA contamination was removed using the
118 TURBO DNA-free Kit (Fisher; # AM1907). mRNA with intact poly(A) tails was enriched using
119 the NEBNext Poly(A) mRNA Magnetic Isolation Module (NEB; # E7490L) and utilized for
120 library constructions with the NEBNext Ultra II Directional RNA Library Prep Kit for Illumina
121 along with NEBNext Multiplex Oligos for Illumina (96 Unique Dual Index Primer Pairs; NEB; #
122 E7760L). The libraries were sequenced on the NovaSeq platform as paired-end reads using the
123 S1 v1.5 kit with 300 cycles (Illumina). FASTQ files were trimmed for adaptor sequences and
124 filtered for low-quality reads using *Trimmomatic*. RNA-seq analysis was conducted as
125 previously described [30-33] with modifications. Briefly, paired-end reads were processed using
126 the *Kallisto* pseudo-alignment method [34] and quantified by mapping to a transcripts database
127 generated from the African Green Monkey (vervet) reference genome assembly (ENSEMBL
128 *Chlorocebus sabaeus* 1.1) [35]. The count table for RNA-seq data was assembled using the
129 *tximport::tximport* function in R. After importing data to the R environment we removed data for
130 genes with low expression using the *edgeR::filterByExpr* function [36]. Normalization was then
131 performed using the *edgeR::calcNormFactors* function, and the *limma::voom* function was used
132 to convert the data into a normal distribution. We calculated differential expression using the
133 *limma::lmFit* function with empirical Bayes moderation via the *limma::eBayes* function (**Table**
134 **S1**). Finally, we performed a gene set enrichment analysis using the *limma::camera* function.
135 Gene set enrichment analysis was conducted using Gene Ontology (GO) annotation for
136 *Chlorocebus sabaeus* obtained from g:Profiler [37]. Raw data were deposited to NCBI
137 BioProject (PRJNA1101086).

138 The following analytical strategy was chosen to normalize for intrinsic transcriptional
139 differences (**Tables S2A-D**) and compare RNA-seq data between Zika virus-infected ZAP-WT
140 cells and Zika virus-infected ZAP-KO cells. Initially, we compared transcriptional responses
141 between non-infected and infected VERO-ZAP-WT cells. Subsequently, we compared
142 transcriptional responses between non-infected and infected VERO-ZAP-KO cells. Finally,
143 genes and GO processes affected by infection were summarized in **Table S2** and figures, and
144 pairwise comparison of genes and comparative GO analysis between VERO-ZAP-WT and
145 VERO-ZAP-KO cells were conducted (**Figs 2-4**; **S2Fig; Table S2**).
146
147 **Statistics**
148 Zika RNA loads, infectious $TCID_{50}$ titers, and CellTiter-Glo Luminescent Assay data in VERO-
149 ZAP-WT and VERO-ZAP-KO cells were compared using an unpaired t-test. A P-value < 0.05
150 was considered statistically significant.
151
152 Experimental details for Zika virus infection kinetics, Western blot, RT-qPCR, cytopathic effect
153 kinetics, and cell viability assay are in supplemental materials and methods.
154
155 **RESULTS**
156 **ZAP affects Zika virus infection phenotypes**
157 We infected VERO-ZAP-WT and VERO-ZAP-KO (**Fig 1A**) with an MOI 1 of Zika virus, and
158 sampled control (4-6 well replicates) and infected (6 well replicates) cells at 24 h and 72 h. We
159 compared intracellular viral RNA loads between WT and ZAP-KO cells with the Zika-specific
160 RT-qPCR. At 24 h post-inoculation, there was no significant difference in Zika virus

161 intracellular RNA loads; however, VERO-ZAP-KO cells showed a trend towards higher RNA
162 loads (**Fig 1B**). At 72 h post-inoculation, Zika virus intracellular RNA loads were significantly
163 higher in VERO-ZAP-KO cells (**Fig 1B**). Expression of Zika virus NS5 protein, as determined
164 by Western blot at 24 h and 72 h (**Fig S1**), corresponded with intracellular RNA loads (**Fig 1B**).
165 However, the effects of ZAP on infection were more pronounced at the viral protein level (**Fig**
166 **S1**). Specifically, at 24 h post-inoculation, Zika NS5 bands were visible in VERO-ZAP-KO
167 cells, while the assay sensitivity was insufficient to detect NS5 in VERO-ZAP-WT cells. By 72 h
168 post-inoculation, Zika NS5 was detected in both VERO-ZAP-KO and VERO-ZAP-WT cells,
169 with protein loads considerably higher in VERO-ZAP-WT cells (**Fig S1**). In addition to Zika
170 intracellular RNA and NS5 WB assays, infectious Zika virus titers in the supernatants of VERO-
171 ZAP-KO cells were significantly higher than VERO-ZAP-WT titers at 24, 48, and 96 hours (**Fig**
172 **1C**).
173

174 **ZAP affects global cellular gene expression during Zika virus infection**

175 How ZAP affects global gene expression in response to virus infection was unknown. Initially,
176 we conducted simple pairwise comparisons of differentially expressed genes (DEGs). First, we
177 compared global gene expression between mock-infected VERO-ZAP-WT and VERO-ZAP-KO
178 cells: 758 and 992 genes were differently expressed between two cell lines at 24 and 72 h (**Fig**
179 **2A**; **Tables S2A, B**). Among the top ten affected genes at 24 h and 72 h (**Table S2A, B**) was
180 only one upregulated gene with known innate immunity or apoptosis function—CXCL12 (**Fig**
181 **2A**). This contrasts with affected top genes in infected cells described below.
182 Second, we compared global gene expression between mock-infected and Zika-infected VERO-
183 ZAP-WT cells: 40 and 117 genes were affected by infection at 24 h and 72 h (**Fig 2B**; **Tables**

184 **S2E, F**). Among the top ten affected genes (**Tables S2E, F**) were four genes with known innate
185 immunity or apoptosis functions—CXCL10, EGR1, G0S2, and CCL2 at 24 h, and seven
186 genes—CCL2, G0S2, CXCL10, IFNL1, OASL, CXCL8, and IL1A at 72 h. All these genes were
187 upregulated in Zika virus-infected ZAP-WT cells (**Fig 2B**).
188 Third, we compared global gene expression between mock-infected and Zika-infected VERO-
189 ZAP-KO cells: 14 and 342 genes were affected by infection at 24 h and 72 h (**Fig 2C**; **Tables**
190 **S2I, J**). Among the top ten affected genes (**Table S2I, J**) were four genes with known innate
191 immunity or apoptosis functions— EGR1, IL1A, FOS, and EGR2 at 24 h, and five genes—
192 G0S2, CCL2, CXCL10, IFNL1, and OASL at 72 h. All these genes were upregulated in Zika
193 virus-infected ZAP-KO cells (**Fig 2C**).
194
195 To further extend analysis beyond pairwise comparisons of top DEGs, we conducted GO
196 analysis. This method offers high sensitivity due to its robust annotation framework,
197 standardized terminology, hierarchical structure, integration with biological knowledge,
198 continuous updates, and statistical rigor where each gene in the entire input set (**Table S1**) is
199 statistically processed and used for annotation [38,39].
200 Along with profound gene expression changes, mock-infected VERO-ZAP-WT and VERO-
201 ZAP-KO cells had 92 (24 h) and 178 (72 h) significantly affected GO biological processes
202 (**Tables S2C, D**). However, when we searched among affected GO biological processes
203 keywords—"viral/virus", "apoptotic/apoptosis", "immun*", and "interferon," we did not find
204 affected processes containing these keywords. This sharply contrasts with affected GO biological
205 processes in infected cells described below. Zika-infected VERO-ZAP-WT cells had 303 (24 h)

206 and 864 (72 h) affected GO biological processes (**Tables S2G, H**). Zika-infected VERO-ZAP-
207 KO cells had 287 (24 h) and 384 (72 h) affected GO biological processes (**Tables S2K, L**).
208 We narrowed down analysis and compared GO biological processes related to virus infection in
209 VERO-ZAP-WT and VERO-ZAP-KO cells at 24 and 72 h. As expected, no affected "viral" GO
210 processes were detected in mock-infected control cells (**Fig 3A**). Infected VERO-ZAP-WT cells
211 showed 5 affected processes at 24 h, and the number increased at 72 h reaching 16 affected
212 processes (**Fig 3B**). In contrast, infected VERO-ZAP-KO cells showed no affected processes at
213 24 h, and the number increased at 72 h reaching only 5 affected processes (**Fig 3C**).
214 We also compared GO biological processes related to immune responses in VERO-ZAP-WT and
215 VERO-ZAP-KO cells at 24 and 72 h. As expected, no affected "immune*" GO processes were
216 detected in mock-infected control cells (**Fig 4A**). Infected VERO-ZAP-WT cells showed one
217 affected process at 24 h, and the number increased at 72 h reaching 16 affected processes (**Fig**
218 **4B**). Infected VERO-ZAP-KO cells showed one affected process at 24 h, and the number
219 increased at 72 h reaching only 4 affected processes (**Fig 4C**).
220 Affected GO biological processes related to apoptosis in VERO-ZAP-WT and VERO-ZAP-KO
221 cells (**Fig S2**) had the same patterns as "viral" and "immune" processes (**Figs 3, 4**). No affected
222 "apoptosis" GO processes were detected in mock-infected control cells (**Fig S2A**). Infected
223 VERO-ZAP-WT cells showed 5 affected processes at 24 h, and the number increased at 72 h
224 reaching 24 affected processes (**Fig S2B**). In contrast, infected VERO-ZAP-KO cells showed
225 only 2 affected processes at 24 h, and the number increased at 72 h reaching only 9 affected
226 processes (**Fig S2C**).
227

228 More aggressive "viral" responses to infection in VERO-ZAP-WT cells than in VERO-ZAP-KO
229 cells at 24 h identified by GO analysis (**Fig 3B**, **C**) may determine the higher number of affected
230 "apoptosis" GO processes in VERO-ZAP-WT cells (**Fig S2B**, **C**) because antiviral
231 transcriptional responses and cell death are interconnected and are critical components of the
232 host response to virus infection [40,41]. Many innate immune signaling pathways can promote
233 cell death [40,41]. In contrast to the signaling pathways that promote antiviral transcription,
234 those that initiate cell death following virus infection remain less understood [40]. To probe
235 whether ZAP affects cell death during Zika infection in VERO cells, we compared cytopathic
236 effects (CPE) in VERO-ZAP-WT and VERO-ZAP-KO cells. We infected VERO-ZAP-WT and
237 VERO-ZAP-KO in the same way as in the RNA-seq experiment with an MOI 1 of Zika virus. At
238 24 h, VERO-ZAP-KO cells did not show visible CPE (**Fig S3**). In contrast, VERO-ZAP-WT
239 cells showed prominent CPE at 24 h—diffuse focies of detached cells (**Fig S3**). At 30 h, the
240 difference was prominent, CPE in VERO-ZAP-WT aggravated to diffuse cell detachment, but
241 VERO-ZAP-KO cells did not display visible CPE until 48 h post-infection (**Fig S3**). At 48 h and
242 72 h, both cell lines had similar diffused cell detachment; however, continuous cell monolayers
243 were mostly preserved. This CPE pattern aggravated at 96 h, where VERO-ZAP-WT had a lot of
244 dead cells but still maintained preserved monolayer, and VERO-ZAP-KO had many dead cells
245 with many spots of disrupted monolayer. At 120 h, the monolayers were mostly disrupted in both
246 cell lines.
247
248
249 The viability patterns of VERO-ZAP-WT and VERO-ZAP-KO cells, as determined by the
250 CellTiter-Glo® Luminescent Cell Viability Assay (**Fig 1D**), showed temporal shifts compared to

251 CPE patterns determined with a microscope (**Fig S3**). Differences in CellTiter-Glo viability were
252 observable starting at 48 h after Zika virus infection, whereas foci of detached cells were visually
253 detectable as early as 24 hours (**Fig S3**). The difference may be explained by distinct
254 methodology principles where CPE is assessed visually versus CellTiter-Glo reagent generating
255 a luminescent signal proportional to the amount of adenosine triphosphate present after chemical
256 cell lysis. The ongoing cell proliferation at 24 h (**Fig 1D**) could potentially impede the ability of
257 the CellTiter-Glo assay to detect dying cells early. Different plate format for assays, 96-well
258 plates for CellTiter-Glo and 6-well plates for CPE, could also contribute to observed differences.
259 Nevertheless, the CellTiter-Glo® Luminescent Cell Viability Assay confirmed general CPE
260 patterns where VERO-ZAP-WT cells had higher CellTiter-Glo mortality at earlier infection (at
261 48 h). Then, mortality between the two cell types equalized (at 72 h), and VERO-ZAP-KO had
262 higher mortality at later infection (96 h and 120 h; P=0.0265 and P=0.0026) (**Fig 1D**).
263
264 Taken together, infection kinetics, RNA-seq data, and cell death patterns support our hypothesis
265 that a more robust, potentially ZAP-mediated, antiviral response in VERO-ZAP-WT cells
266 compared to VERO-ZAP-KO cells (**Figs 3, 4; Fig S2**) more effectively controls Zika virus
267 infection (**Figs 1B, C**; **Fig S1**), but leads to heightened cell death during early infection (24-48 h;
268 **Fig 1D; Fig S3**) because many innate immune signaling pathways can promote cell death
269 [40,41]. Afterward, the less controlled infection in ZAP-KO cells at 72 h (**Figs 1B, C; Fig S1**)
270 may contribute to more extensive cell lysis at later time infection (96-120 h) (**Fig 1D; Fig S3**).
271 Further studies are needed to validate this hypothesis and gain a better understanding of the
272 molecular interplay between ZAP-mediated antiviral responses and cell death.
273

274 **DISCUSSION**

275 The zinc finger CCCH-type antiviral protein 1 is an interferon (IFN)-stimulated gene (ISG) [1-
276 5]. Also, there are conflicting studies regarding the capacity of ZAP to enhance the type I IFN
277 antiviral response [5,42-44]. Here, we found that during Zika infection, endogenous ZAP was
278 associated with amplification of global transcriptional antiviral and immune responses in VERO
279 cells which are deficient in IFN-α/β [4,45]. We do not know yet how these type I IFN-
280 independent antiviral cellular responses associated with endogenous ZAP work. ZAP knockout
281 also considerably impacted global gene expression in uninfected cells; however, GO processes
282 related to antiviral, immune, and apoptosis events were not identified, suggesting the specificity
283 of findings in Zika-infected cells.

284

285 Our study is confined to a single VERO-ZAP-KO clone, and conducting additional tests using
286 multiple clones could yield further insights. Such an endeavor falls beyond the scope of this
287 study; however, our RNA-seq results find indirect support from previous research conducted on
288 different uninfected wild-type and ZAP-KO cell lines. Specifically, global gene expression
289 analysis with Agilent microarrays revealed 1,065 upregulated and 776 downregulated transcripts
290 in uninfected wild-type and ZAP-KO HeLa cells [46]. Another study using RNA-seq identified a
291 number of DEGs between uninfected ZAP-WT and ZAP-KO A549 cells [47]. In the most recent
292 study, the authors demonstrated that ZAP influences hundreds of transcripts in ZAP-WT and
293 ZAP-KO HEK cells [48]. Directly comparing the DEGs between our study and the above studies
294 poses challenges due to variations in cell types, experimental design, and the employed
295 bioinformatics. Nonetheless, the overarching trend in all previous studies strongly corroborates

296 significant transcriptional differences between non-infected ZAP-WT and ZAP-KO VERO cells
297 (**Fig 2A; Tables S2A-D**).
298
299 The above studies did not use virus infection for RNA-seq comparison between ZAP-WT and
300 ZAP-KO cells. Thus, our study provides the first high-throughput dataset highlighting the impact
301 of ZAP on global gene expression during virus infection. During submission of this manuscript,
302 a study indirectly supporting our findings was published [48]. The authors used RNA-seq in
303 ZAP-WT and ZAP-KO HEK cells transfected with viral mimetic RNA oligos and mock
304 transfection to normalize DEGs. From this study, we used the top 16 innate immune response
305 genes (**Table S2M**) overexpressed in ZAP-WT HEK cells as compared to ZAP-KO for
306 comparative purposes. At 24 h, two genes in this HEK list (**Table S2M**)—IFIT1 and ISG15—
307 were upregulated in Zika virus-infected VERO-ZAP-WT cells as compared to mock control
308 VERO-ZAP-WT cells (**Table S2E;** highlighted). In contrast, no genes from the HEK list were
309 affected in Zika virus-infected VERO-ZAP-KO cells (**Table S2I**). At 72 h, eight-nine innate
310 immune response genes in the list (**Table S2M**) were upregulated in both Zika virus-infected
311 VEO-ZAP-WT and VERO-ZAP-KO cells (**Table S2F, J**); but comparison at 72 h is not
312 sufficiently informative because previous HEK study was only conducted at 24 h after
313 transfection. Nonetheless, this pattern of ZAP-dependent affected genes, where ZAP-WT cells
314 show innate immune responses earlier than ZAP-KO cells, is in accordance with our GO analysis
315 (**Figs 3, 4**).
316 We do not see a complete match between the previous HEK (**Table S2M**) and our VERO
317 dataset; not all genes identified as upregulated in transfected ZAP-WT HEK cells were
318 significantly upregulated in infected VERO-ZAP-WT cells (**Table S2E, I, F, J**). This

319 discrepancy may be explained by different approaches (transfection versus infection), the type I
320 IFN competency of HEK cells, and the deficiency of VERO cells. Nonetheless, two important
321 innate immune genes—IFIT1 and ISG15—were upregulated in transfected or infected ZAP-WT
322 cells in both studies, suggesting their ZAP-mediated augmentation in the absence of the type I
323 IFN system. Potential type I IFN-independent and -dependent interactions between ZAP and
324 IFIT1 are of interest because ZAP and IFIT1 together have recently been identified to constitute
325 the majority of IFN-mediated restriction of alphavirus, specifically Venezuelan equine
326 encephalitis virus [26].
327
328 The previous ZAP study showed JEV sensitivity to ectopic ZAP, and insensitivity of Zika virus
329 [7]. The discrepancy between previous and present studies may be explained by different
330 experimental approaches. The previous study involved the overexpression of ectopic ZAP in
331 ZAP-positive cells [7], whereas our study compared Zika RNA loads between ZAP-WT and
332 ZAP-KO cells. Additionally, different cell lines were used: A549 cells from human cancer lung
333 tissue in the previous study [7], and VERO cells from a healthy monkey in our study. Antiviral
334 signaling can vary significantly between different cell types [2,49]. Another potential factor is
335 that human cells were used previously, and here we used the cell line derived from a healthy
336 adult African green monkey—a possible natural reservoir host of Zika virus [50]. Moreover,
337 while the previous study used 10 h and 24 h sampling times, we conducted the RT-qPCR,
338 Western blot, and end point dilution $TCID_{50}$ assay for infectious titers at 24-120 h after Zika
339 infection, revealing delayed effects, indicative of indirect ZAP-mediated antiviral activity.
340
341

342 **CONCLUSIONS**

343 Altogether, our preliminary study underscores the importance of ZAP in augmenting cellular
344 responses against Zika virus even in the absence of the robust type I IFN system. Further
345 investigations are warranted to elucidate the mechanisms underlying these type I IFN-
346 independent antiviral cellular responses mediated by ZAP. The considerable augmentation of
347 antiviral responses by endogenous ZAP against Zika virus highlights its potential as a therapeutic
348 target. However, comprehensive studies are required to fully understand the intricacies of ZAP-
349 mediated antiviral activity and its implications for combating Zika virus infection.

350

351 **DISCLOSURE STATEMENT**

352 The authors declare that the research was conducted in the absence of any commercial or
353 financial relationships that could be construed as a potential conflict of interest.

354

355 **DATA AVAILABILITY**

356 Raw RNA-seq files are deposited to NCBI BioProject (PRJNA1101086).

357

358 **FUNDING**

359 PPS received a Scholarship from the School of Public Health, University of Saskatchewan. This
360 work was partially supported by a grant to UK from the Canadian Institutes of Health Research
361 (CIHR; Project Grant #424307). The funders had no role in study design, data collection and
362 analysis, decision to publish, or manuscript preparation.

363

364

365 **REFERENCES**

366 1. Nguyen LP, Aldana KS, Yang E, et al. Alphavirus Evasion of Zinc Finger Antiviral Protein (ZAP)
367 Correlates with CpG Suppression in a Specific Viral nsP2 Gene Sequence. Viruses. 2023 Mar
368 24;15(4).
369 2. MacDonald MR, Machlin ES, Albin OR, et al. The zinc finger antiviral protein acts synergistically
370 with an interferon-induced factor for maximal activity against alphaviruses. J Virol. 2007
371 Dec;81(24):13509-18.
372 3. Li MMH, Aguilar EG, Michailidis E, et al. Characterization of Novel Splice Variants of Zinc Finger
373 Antiviral Protein (ZAP). J Virol. 2019 Sep 15;93(18).
374 4. Crosse KM, Monson EA, Beard MR, et al. Interferon-Stimulated Genes as Enhancers of Antiviral
375 Innate Immune Signaling. J Innate Immun. 2018;10(2):85-93.
376 5. Hayakawa S, Shiratori S, Yamato H, et al. ZAPS is a potent stimulator of signaling mediated by
377 the RNA helicase RIG-I during antiviral responses. Nat Immunol. 2011 Jan;12(1):37-44.
378 6. Zhu Y, Gao G. ZAP-mediated mRNA degradation. RNA Biol. 2008 Apr-Jun;5(2):65-7.
379 7. Chiu HP, Chiu H, Yang CF, et al. Inhibition of Japanese encephalitis virus infection by the host
380 zinc-finger antiviral protein. PLoS Pathogens: Public Library of Science; 2018.
381 8. Ye P, Liu S, Zhu Y, et al. DEXH-Box protein DHX30 is required for optimal function of the zinc-
382 finger antiviral protein. Protein Cell. 2010 Oct;1(10):956-64.
383 9. Chen G, Guo X, Lv F, et al. p72 DEAD box RNA helicase is required for optimal function of the
384 zinc-finger antiviral protein. Proc Natl Acad Sci U S A. 2008 Mar 18;105(11):4352-7.
385 10. Li MM, Lau Z, Cheung P, et al. TRIM25 Enhances the Antiviral Action of Zinc-Finger Antiviral
386 Protein (ZAP). PLoS Pathog. 2017 Jan;13(1):e1006145.
387 11. Zheng X, Wang X, Tu F, et al. TRIM25 Is Required for the Antiviral Activity of Zinc Finger Antiviral
388 Protein. Journal of virology: J Virol; 2017.
389 12. Ficarelli M, Wilson H, Pedro Galão R, et al. KHNYN is essential for the zinc finger antiviral protein
390 (ZAP) to restrict HIV-1 containing clustered CpG dinucleotides. eLife2019.
391 13. Buckmaster MV, Goff SP. Riplet Binds the Zinc Finger Antiviral Protein (ZAP) and Augments ZAP-
392 Mediated Restriction of HIV-1. Journal of Virology: American Society for Microbiology; 2022.
393 14. Gao G, Guo X, Goff SP. Inhibition of retroviral RNA production by ZAP, a CCCH-type zinc finger
394 protein. Science (New York, N.Y.): American Association for the Advancement of Science; 2002.
395 p. 1703-6.
396 15. Bick MJ, Carroll JW, Gao G, et al. Expression of the zinc-finger antiviral protein inhibits alphavirus
397 replication. J Virol. 2003 Nov;77(21):11555-62.
398 16. Liu CH, Zhou L, Chen G, et al. Battle between influenza A virus and a newly identified antiviral
399 activity of the PARP-containing ZAPL protein. Proc Natl Acad Sci U S A. 2015 Nov
400 10;112(45):14048-53.
401 17. Mao R, Nie H, Cai D, et al. Inhibition of hepatitis B virus replication by the host zinc finger
402 antiviral protein. PLoS Pathog. 2013;9(7):e1003494.
403 18. Muller S, Moller P, Bick MJ, et al. Inhibition of filovirus replication by the zinc finger antiviral
404 protein. J Virol. 2007 Mar;81(5):2391-400.
405 19. Tang Q, Wang X, Gao G. The Short Form of the Zinc Finger Antiviral Protein Inhibits Influenza A
406 Virus Protein Expression and Is Antagonized by the Virus-Encoded NS1. J Virol. 2017 Jan
407 15;91(2).
408 20. Zhu Y, Chen G, Lv F, et al. Zinc-finger antiviral protein inhibits HIV-1 infection by selectively
409 targeting multiply spliced viral mRNAs for degradation. Proc Natl Acad Sci U S A. 2011 Sep
410 20;108(38):15834-9.

411 21. Takata MA, Goncalves-Carneiro D, Zang TM, et al. CG dinucleotide suppression enables antiviral
412 defence targeting non-self RNA. Nature. 2017 Oct 5;550(7674):124-127.
413 22. Miyazato P, Matsuo M, Tan BJY, et al. HTLV-1 contains a high CG dinucleotide content and is
414 susceptible to the host antiviral protein ZAP. Retrovirology. 2019 Dec 16;16(1):38.
415 23. Gonzalez-Perez AC, Stempel M, Wyler E, et al. The Zinc Finger Antiviral Protein ZAP Restricts
416 Human Cytomegalovirus and Selectively Binds and Destabilizes Viral UL4/UL5 Transcripts. mBio.
417 2021 May 4;12(3).
418 24. Zhao Y, Song Z, Bai J, et al. ZAP, a CCCH-Type Zinc Finger Protein, Inhibits Porcine Reproductive
419 and Respiratory Syndrome Virus Replication and Interacts with Viral Nsp9. J Virol. 2019 May
420 15;93(10).
421 25. Xie L, Lu B, Zheng Z, et al. The 3C protease of enterovirus A71 counteracts the activity of host
422 zinc-finger antiviral protein (ZAP). J Gen Virol. 2018 Jan;99(1):73-85.
423 26. McDougal MB, De Maria AM, Ohlson MB, et al. Interferon inhibits a model RNA virus via a
424 limited set of inducible effector genes. EMBO Rep. 2023 Sep 6;24(9):e56901.
425 27. Trus I, Udenze D, Berube N, et al. CpG-Recoding in Zika Virus Genome Causes Host-Age-
426 Dependent Attenuation of Infection With Protection Against Lethal Heterologous Challenge in
427 Mice. Front Immunol. 2019;10:3077.
428 28. Trus I, Berube N, Jiang P, et al. Zika Virus with Increased CpG Dinucleotide Frequencies Shows
429 Oncolytic Activity in Glioblastoma Stem Cells. Viruses: Multidisciplinary Digital Publishing
430 Institute; 2020. p. 579.
431 29. Udenze D, Trus I, Berube N, et al. The African strain of Zika virus causes more severe in utero
432 infection than Asian strain in a porcine fetal transmission model. Emerging Microbes &
433 Infections. 2019; 8:1098-1107.2019.
434 30. Darbellay J, Cox B, Lai K, et al. Zika Virus Causes Persistent Infection in Porcine Conceptuses and
435 may Impair Health in Offspring. EBioMedicine. 25:73-86.2017.
436 31. Trus I, Udenze D, Cox B, et al. Subclinical in utero Zika virus infection is associated with
437 interferon alpha sequelae and sex-specific molecular brain pathology in asymptomatic porcine
438 offspring. In: Pierson TC, editor. PLoS Pathogens2019. p. e1008038.
439 32. Udenze D, Trus I, Lipsit S, et al. Offspring affected with in utero Zika virus infection retain
440 molecular footprints in the bone marrow and blood cells. Emerging microbes & infections:
441 Emerg Microbes Infect; 2022. p. 1-43.
442 33. Chapagain S, Pal Singh P, Le K, et al. Japanese encephalitis virus persists in the human
443 reproductive epithelium and porcine reproductive tissues. PLoS Negl Trop Dis. 2022
444 Jul;16(7):e0010656.
445 34. Bray NL, Pimentel H, Melsted P, et al. Near-optimal probabilistic RNA-seq quantification. Nature
446 Biotechnology. 2016 2016/05/01;34(5):525-527.
447 35. Warren WC, Jasinska AJ, Garcia-Perez R, et al. The genome of the vervet (Chlorocebus aethiops
448 sabaeus). Genome Res. 2015 Dec;25(12):1921-33.
449 36. Law CW, Alhamdoosh M, Su S, et al. RNA-seq analysis is easy as 1-2-3 with limma, Glimma and
450 edgeR. F1000Res. 2016;5.
451 37. Raudvere U, Kolberg L, Kuzmin I, et al. g:Profiler: a web server for functional enrichment analysis
452 and conversions of gene lists (2019 update). Nucleic Acids Res. 2019 Jul 2;47(W1):W191-W198.
453 38. The Gene Ontology C. The Gene Ontology Resource: 20 years and still GOing strong. Nucleic
454 Acids Res. 2019 Jan 8;47(D1):D330-D338.
455 39. Ashburner M, Ball CA, Blake JA, et al. Gene ontology: tool for the unification of biology. The
456 Gene Ontology Consortium. Nat Genet. 2000 May;25(1):25-9.
457 40. Orzalli MH, Kagan JC. Apoptosis and Necroptosis as Host Defense Strategies to Prevent Viral
458 Infection. Trends Cell Biol. 2017 Nov;27(11):800-809.

459 41. Upton JW, Chan FK. Staying alive: cell death in antiviral immunity. Mol Cell. 2014 Apr
460 24;54(2):273-80.
461 42. Schwerk J, Soveg FW, Ryan AP, et al. RNA-binding protein isoforms ZAP-S and ZAP-L have distinct
462 antiviral and immune resolution functions. Nat Immunol. 2019 Dec;20(12):1610-1620.
463 43. Lee H, Komano J, Saitoh Y, et al. Zinc-finger antiviral protein mediates retinoic acid inducible
464 gene I-like receptor-independent antiviral response to murine leukemia virus. Proc Natl Acad Sci
465 U S A. 2013 Jul 23;110(30):12379-84.
466 44. Kozaki T, Takahama M, Misawa T, et al. Role of zinc-finger anti-viral protein in host defense
467 against Sindbis virus. Int Immunol. 2015 Jul;27(7):357-64.
468 45. Emeny JM, Morgan MJ. Regulation of the interferon system: evidence that Vero cells have a
469 genetic defect in interferon production. J Gen Virol. 1979 Apr;43(1):247-52.
470 46. Todorova T, Bock FJ, Chang P. PARP13 regulates cellular mRNA post-transcriptionally and
471 functions as a pro-apoptotic factor by destabilizing TRAILR4 transcript. Nature communications.
472 2014 Nov 10;5:5362.
473 47. Shaw AE, Rihn SJ, Mollentze N, et al. The antiviral state has shaped the CpG composition of the
474 vertebrate interferome to avoid self-targeting. PLoS Biol. 2021 Sep;19(9):e3001352.
475 48. Busa VF, Ando Y, Aigner S, et al. Transcriptome regulation by PARP13 in basal and antiviral states
476 in human cells. iScience. 2024 Apr 19;27(4):109251.
477 49. Pallett MA, Lu Y, Smith GL. DDX50 Is a Viral Restriction Factor That Enhances IRF3 Activation.
478 Viruses. 2022 Feb 3;14(2).
479 50. Buechler CR, Bailey AL, Weiler AM, et al. Seroprevalence of Zika Virus in Wild African Green
480 Monkeys and Baboons. mSphere. 2017 Mar-Apr;2(2).

481

482

483

484

485

486

487

488

489

490 **FIGURE LEGENDS**

491

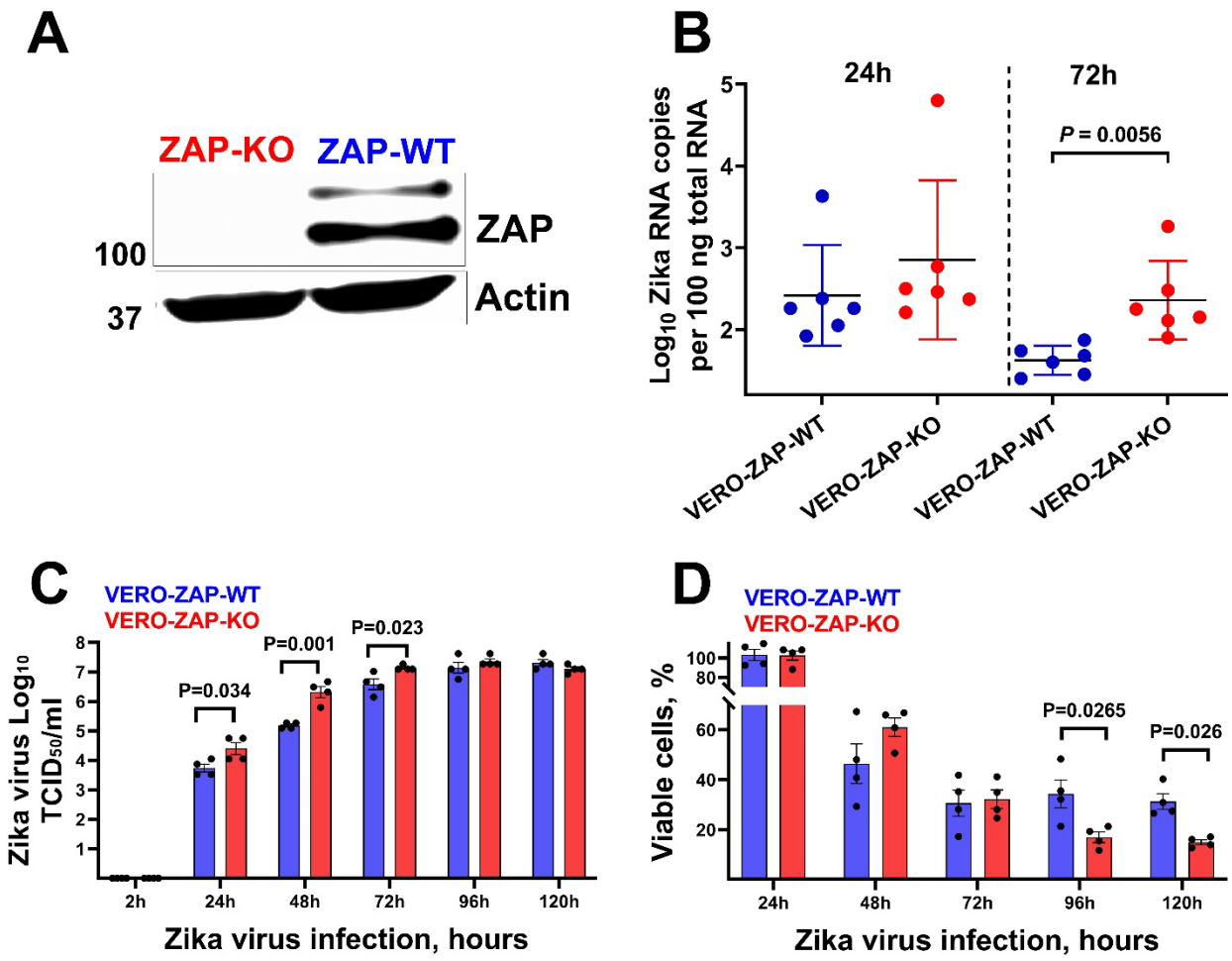

492

493 **Fig 1. Infection phenotypes of Zika virus and cell viability in wild-type (VERO-ZAP-WT)**
494 **and ZAP knockout (VERO-ZAP-KO) cells.** (**A**) ZAP western blot. KO status was also
495 confirmed by Sanger sequencing. (**B**) Reduced intracellular Zika virus RNA in VERO-ZAP-WT
496 cells at 24 h and 72 h after inoculation, MOI 1. Determined by the Zika-specific RT-qPCR assay.
497 All mock-infected samples were negative by Zika-specific RT-qPCR. Statistics—an unpaired t-
498 test. (**C**) Zika virus infectious titers in supernatants of VERO-ZAP-WT and VERO-ZAP-KO cells
499 at different times after inoculation, MOI 1. The experiment was done in four replicates for each
500 cell line and sampling time. Supernatants from all mock-infected samples were negative. (**D**) The
501 CellTiter-Glo Luminescent Assay. The assay was performed in four biological and three technical
502 replicates. Dots represent biological replicates; each biological replicate represents an average of
503 three technical replicates. Statistics—an unpaired t-test.

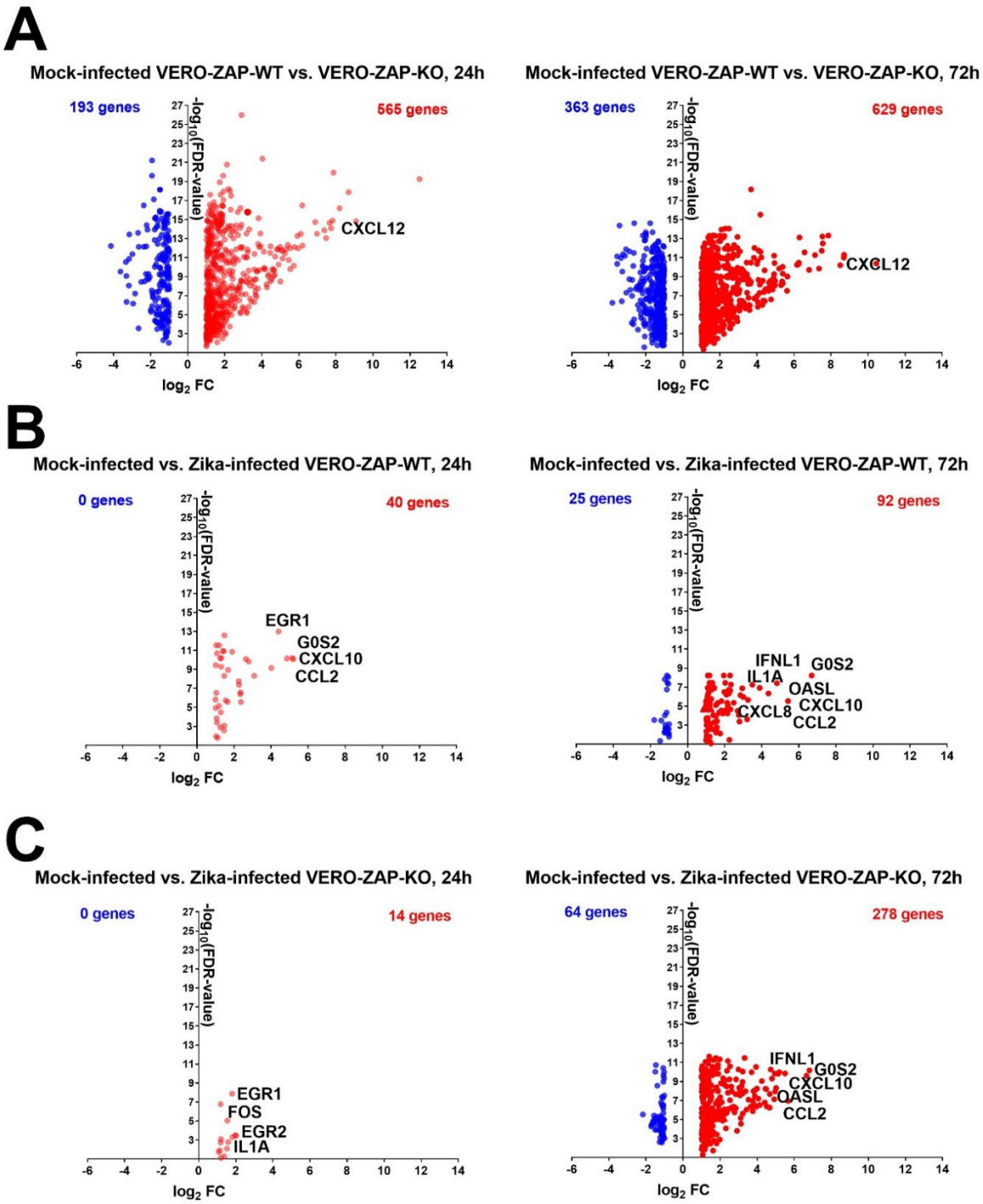

Fig 2. Cellular transcriptional gene responses during Zika virus infection. (**A**) Mock-infected VERO ZAP-WT versus VERO-ZAP-KO cells. Direction of analysis: WT/KO. (**B**) Mock-infected versus Zika-infected VERO-ZAP-WT cells. Direction of analysis: Zika-infected/Mock-infected. (**C**) Mock-infected versus Zika-infected VERO-ZAP-KO cells. Direction of analysis: Zika-infected/Mock-infected. Plots of the upregulated (red) and downregulated (blue) genes. **FDR**: The false discovery rate. Genes with FDR < 0.05 and log2 fold change (FC) > 1 were significantly affected. The top 10 affected genes associated with innate immune response or apoptosis are shown. Raw data are in **Tables S2A, B, E, F, I, J**.

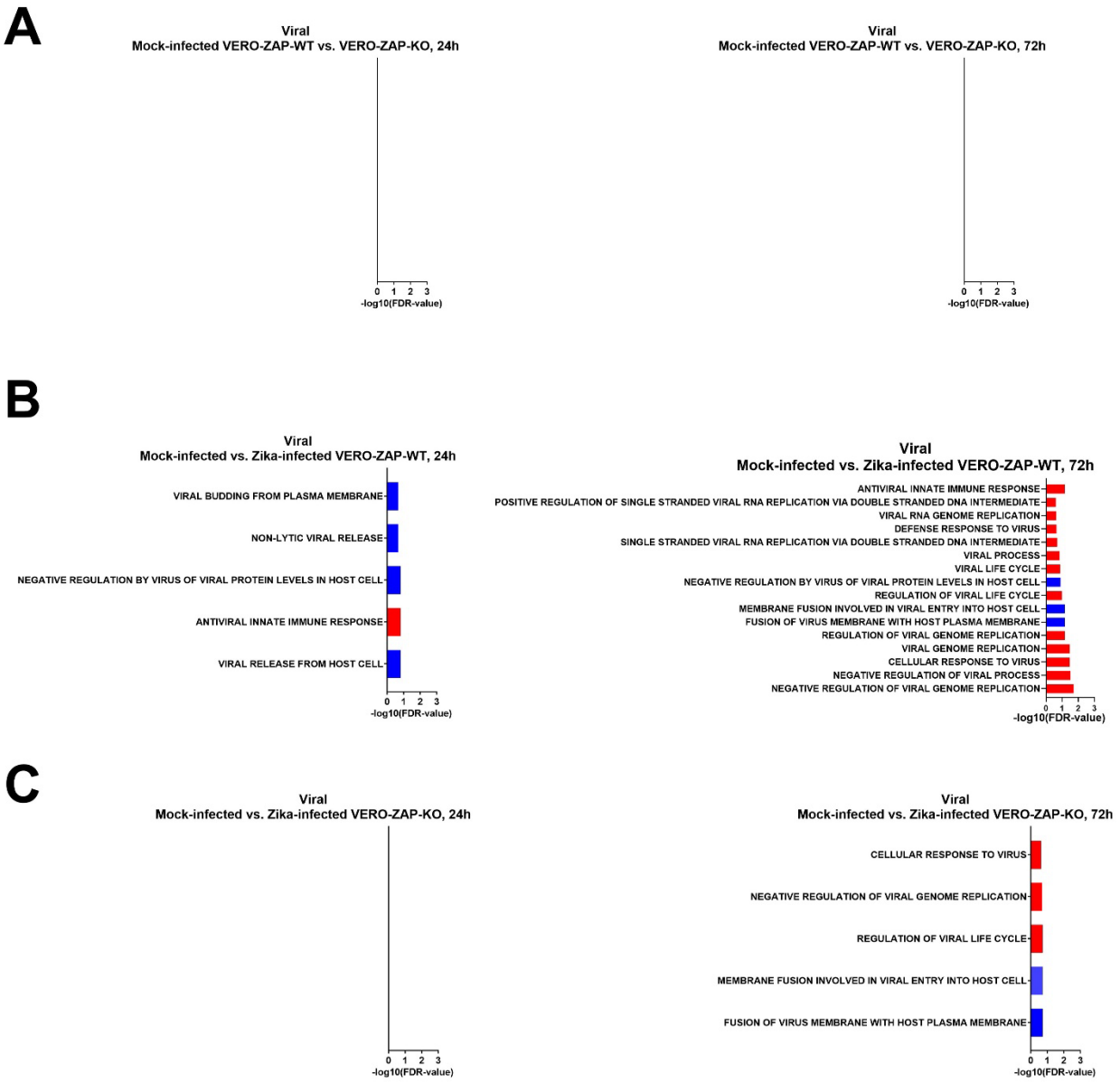

Fig 3. Biological "viral" processes affected in VERO-ZAP-WT and VERO-ZAP-KO cells at 24 h and 72 h after Zika virus infection. (**A**) Mock-infected ZAP-WT versus VERO-ZAP-KO cells. Direction of analysis: WT/KO. (**B**) Mock-infected versus Zika-infected VERO-ZAP-WT cells. Direction of analysis: Zika-infected/Mock-infected. (**C**) Mock-infected versus Zika-infected VERO-ZAP-KO cells. Direction of analysis: Zika-infected/Mock-infected. Red bars–upregulated processes. Blue bars–downregulated processes. **FDR**: The false discovery rate. Raw data are in **Tables S2C, D, G, H, K, L**.

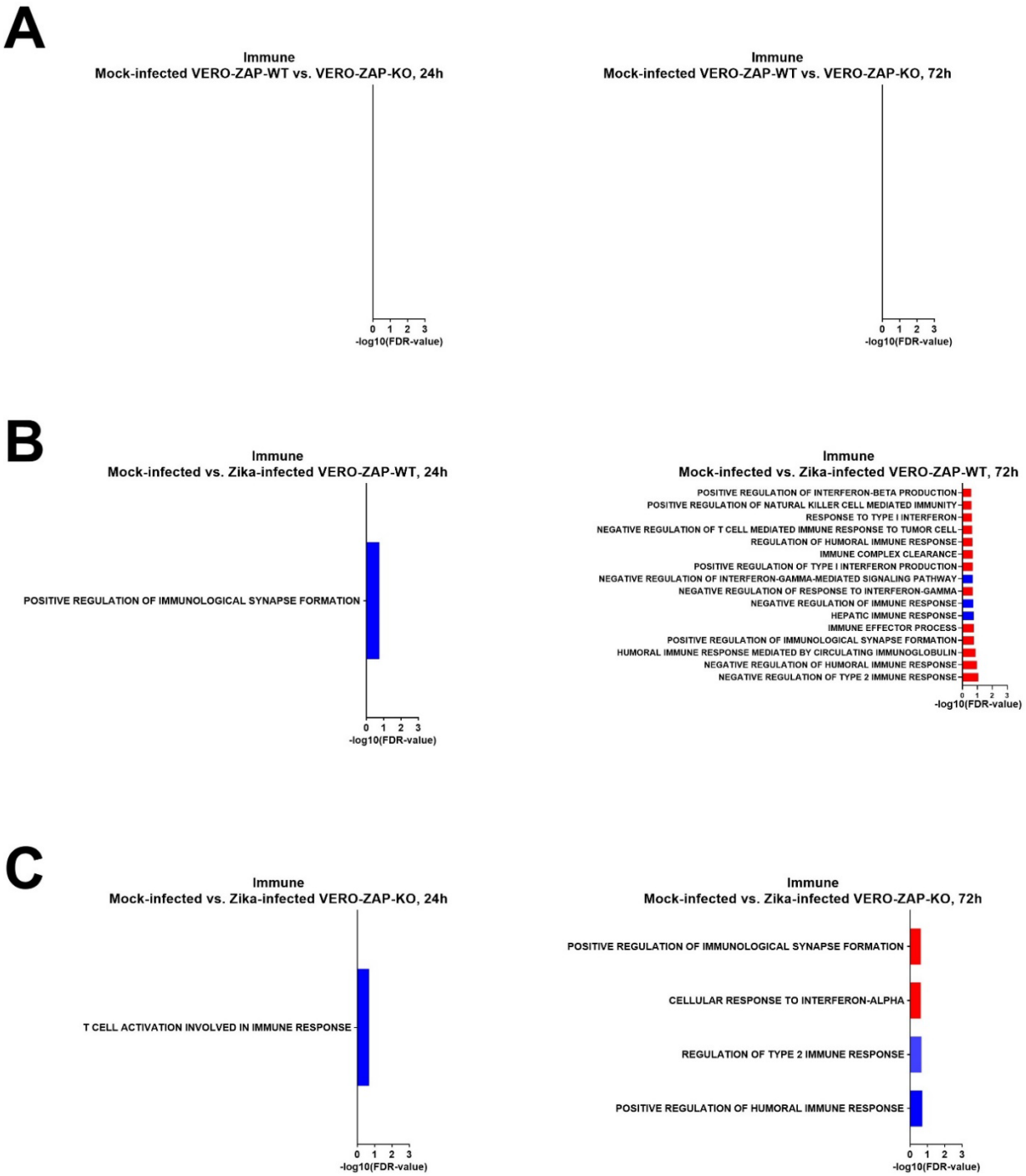

Fig 4. Biological "immune*" processes affected in VERO-ZAP-WT and VERO-ZAP-KO cells at 24 h and 72 h after Zika virus infection. (**A**) Mock-infected ZAP-WT versus VERO-ZAP-KO cells. Direction of analysis: WT/KO. (**B**) Mock-infected versus Zika-infected VERO-ZAP-WT cells. Direction of analysis: Zika-infected/Mock-infected. (**C**) Mock-infected versus Zika-infected VERO-ZAP-KO cells. Direction of analysis: Zika-infected/Mock-infected. Red bars–upregulated processes. Blue bars– downregulated processes. **FDR**: The false discovery rate. Raw data are in **Tables S2C, D, G, H, K, L**.

536 **SUPPLEMENTARY FIGURES**

537

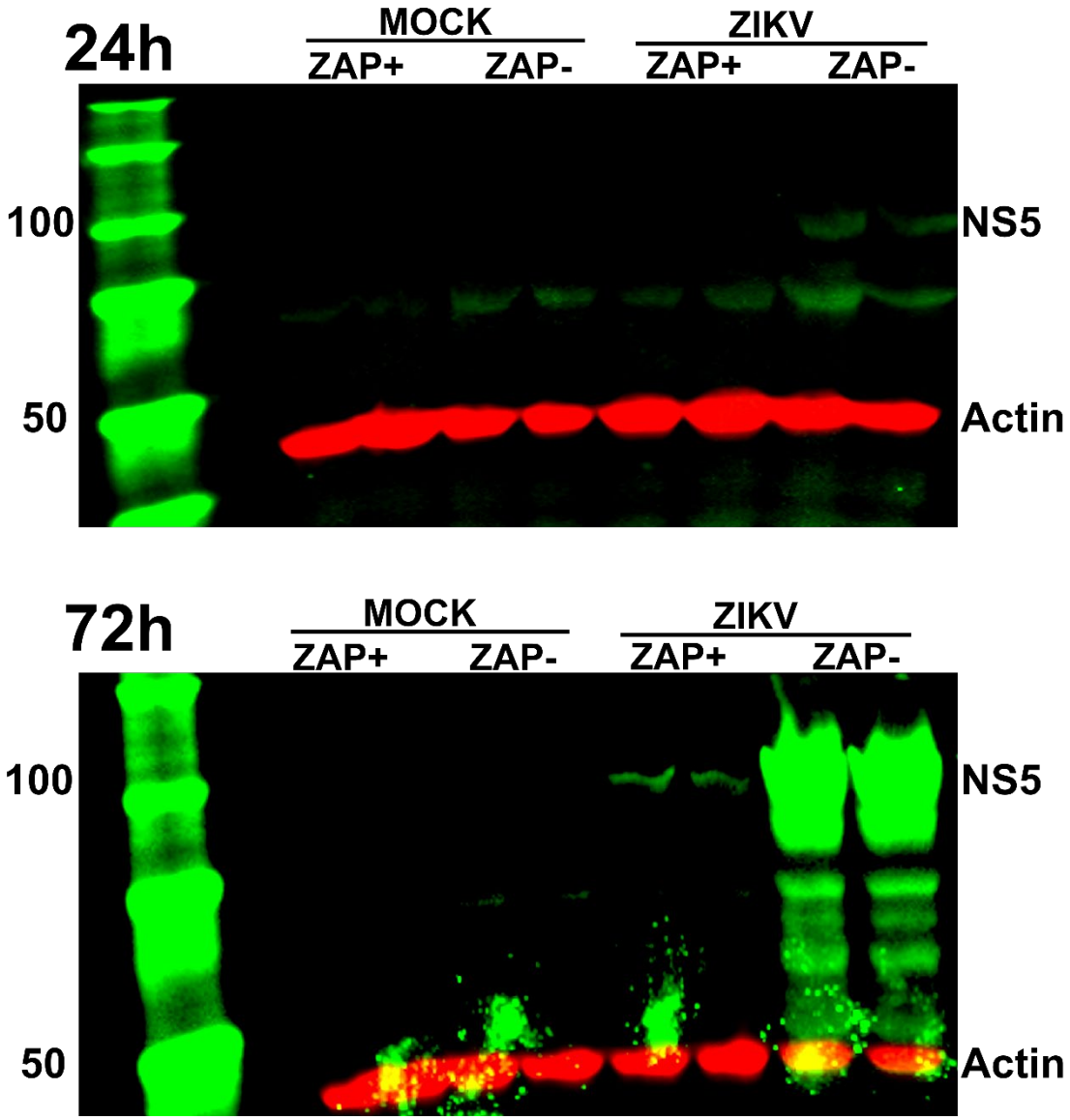

538

539

540 **Fig S1. Zika virus NS5 protein Western blot.** Reduced Zika virus NS5 protein loads in VERO-
541 ZAP-WT cells as compared to VERO-ZAP-KO cells at 24 h and 72 h after inoculation, MOI 1.
542 Rabbit anti-Zika virus NS5 IgG Abs (1:1,000 dilution; GTX133312, GeneTex), with the specific
543 NS5 band appearing at 103 kDa, were used. Beta-actin was used as a western blot loading
544 control (42 kDa, red bands). A normalized 50 µg of protein was used for all samples. Two
545 biological replicates for each condition are shown.

546

547

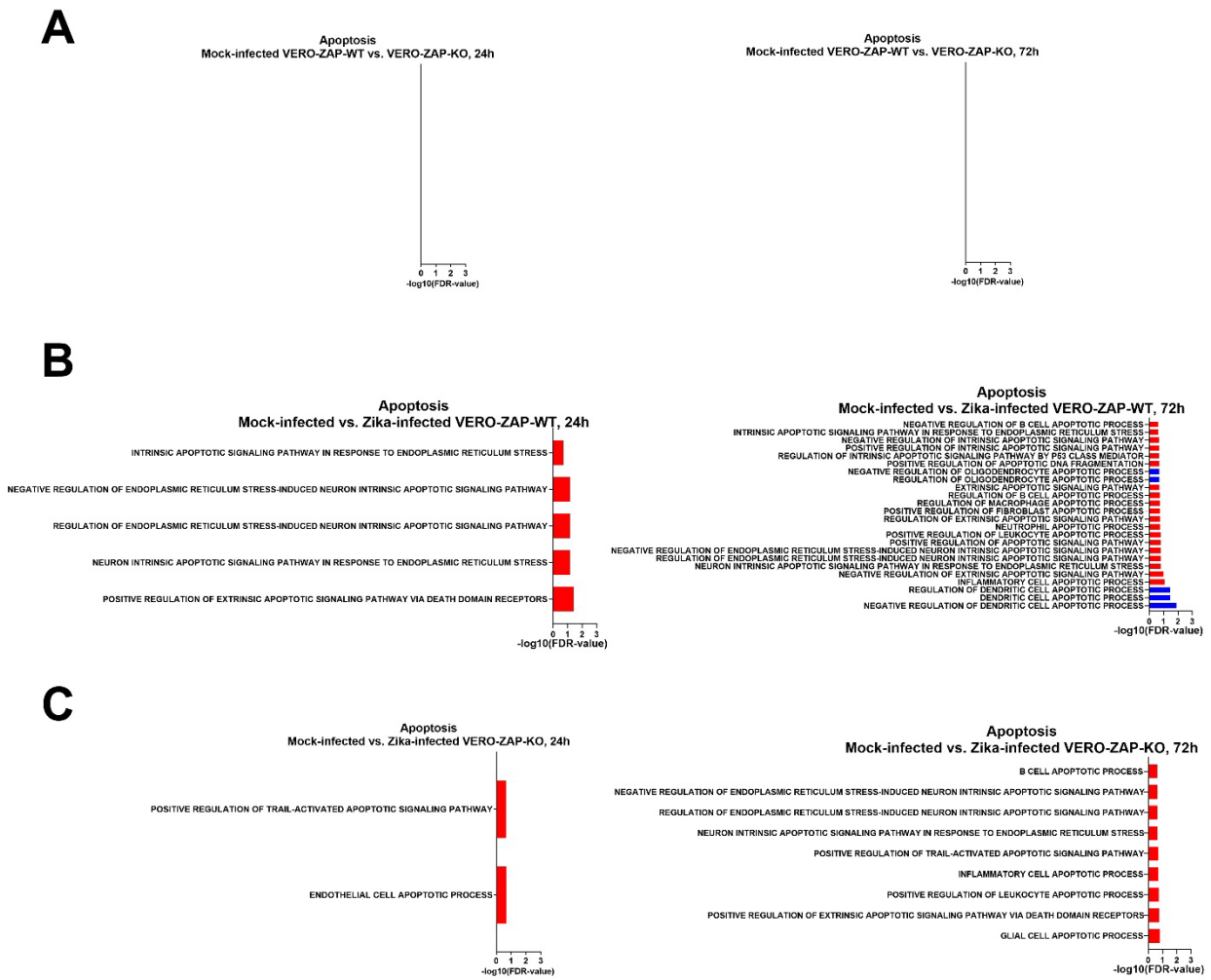

Fig S2. Biological "apoptosis" processes affected in VERO-ZAP-WT and VERO-ZAP-KO cells at 24 h and 72 h after Zika virus infection. (**A**) Mock-infected ZAP-WT versus VERO-ZAP-KO cells. Direction of analysis: WT/KO. (**B**) Mock-infected versus Zika-infected VERO-ZAP-WT cells. Direction of analysis: Zika-infected/Mock-infected. (**C**) Mock-infected versus Zika-infected VERO-ZAP-KO cells. Direction of analysis: Zika-infected/Mock-infected. Red bars–upregulated processes. Blue bars- downregulated processes. **FDR**: The false discovery rate. Raw data are in **Tables S2C, D, G, H, K, L**.

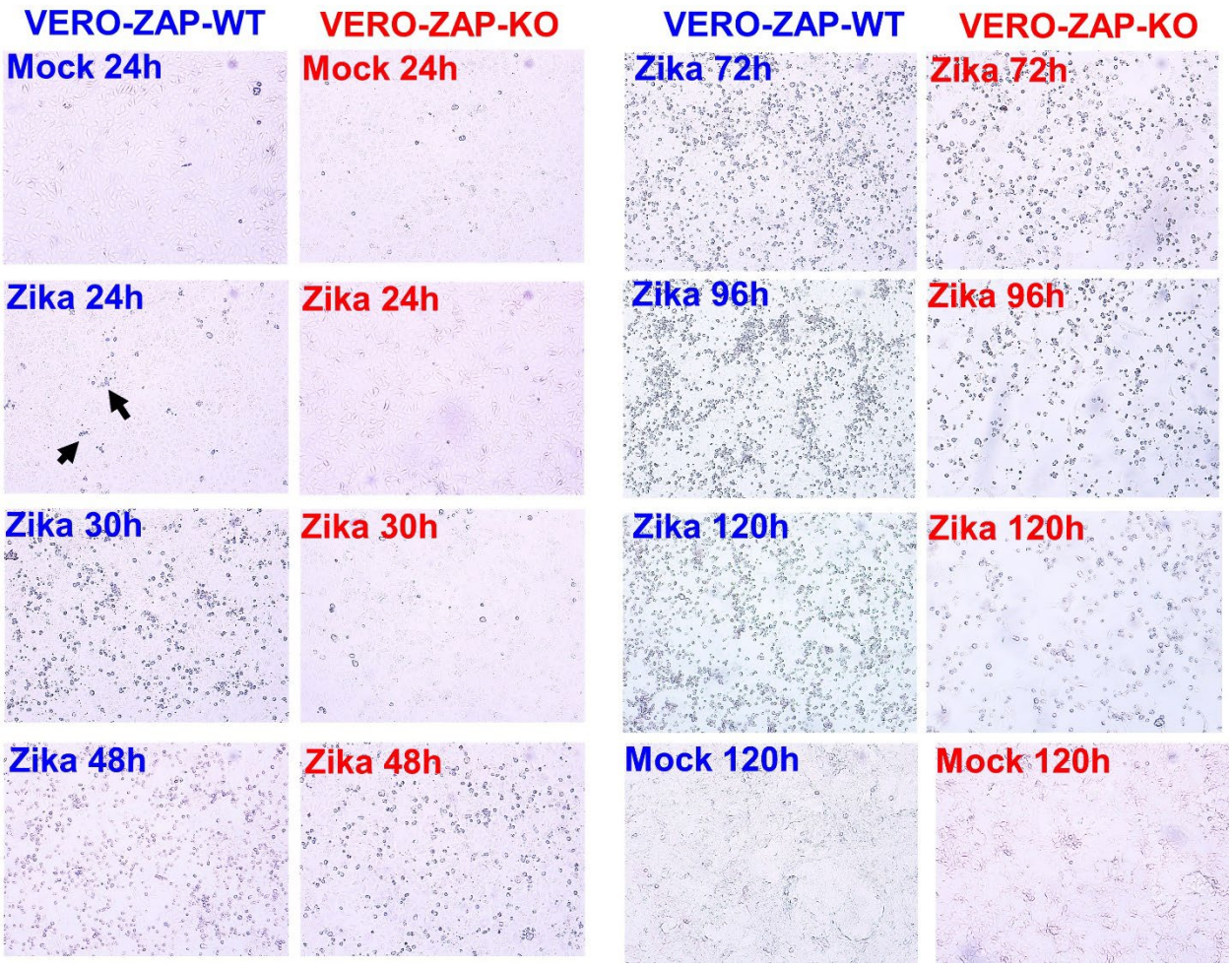

Fig S3. Cytopathic effect patterns during Zika virus infection in VERO-ZAP-WT and VERO-ZAP-KO cells, MOI 1. Arrows show diffuse small focies of detached cells. The experiment was done in three replicates for each cell line. Images represent the typical pattern in all replicates.

Table S1 Raw RNAseq data (DEGs).

Table S2 Significantly affected DEGs and GO processes.

Supplemental Materials and Methods

Endogenous ZAP is associated with altered global cellular gene expression during Zika virus infection

Nguyen Phuong Khanh Le[1], Prince Pal Singh[1,2], Ahmad Jawad Sabir[3], Ivan Trus[4], Uladzimir Karniychuk[1,*]

[1]Department of Veterinary Biosciences, College of Veterinary Medicine, The Ohio State University, Columbus, OH, USA

[2]School of Public Health, University of Saskatchewan, Saskatoon, Canada

[3]Department of Microbiology and Immunology, University of Illinois, College of Medicine, Chicago, IL, USA

[4]Dioscuri Centre for RNA-Protein Interactions in Human Health and Disease, International Institute of Molecular and Cell Biology, Warsaw, Poland

*** Correspondence:** Uladzimir Karniychuk

Department of Veterinary Biosciences, College of Veterinary Medicine, The Ohio State University, Columbus, OH, USA

karniychuk.1@osu.edu

24 **Zika virus infection kinetics**

25 VERO-ZAP-WT and VERO-ZAP-KO cells were seeded in 6-well plates in DMEM
26 supplemented with 10% inactivated fetal bovine serum for 24 h. Four wells for each cell line,
27 representing four biological replicates, were inoculated with Zika virus at a multiplicity of
28 infection (MOI) of 1. After 2 h at 37ºC, the inoculum was removed, the cells were washed three
29 times, covered with 3 ml of DMEM supplemented with 2% FBS, and maintained at 37ºC. At 2,
30 24, 48, 72, 96, and 120 h post-inoculation, 150 µl of media supernatants were collected, cleared
31 by centrifugation, and frozen at -80°C for the end-point dilution $TCID_{50}$ assay [1-6].

32

33 **Western blot**

34 Not manipulated, mock-infected, or Zika-infected (MOI 1) VERO-ZAP-WT and VERO-ZAP-
35 KO cells cultured in T-75 or T-175 flasks were washed, pelletized, and lysed in 300 µL of RIPA
36 buffer (Fisher; # PI89900) supplemented with 1× Halt protease inhibitor cocktail (Fisher;
37 #PI87786) and 1× EDTA (Fisher; #BP2473100). The lysates were then incubated on wet ice for
38 10 minutes, gently vortexed, and centrifuged (12,000g, 10 min, +4 °C). Supernatants were
39 aliquoted into prechilled low protein-binding (Sarstedt; #72.706.600) and stored at -80°C. After
40 quantifying protein concentration with the Pierce BCA Protein Assay Kit (Fisher; # PI23227), 50
41 µg of protein extract was diluted in 4× reducing Laemmli SDS sample buffer (Fisher;
42 #AAJ60015AC), heated at 95ºC for 10 min, and resolved on 10% Mini-PROTEAN TGX precast
43 protein gels (Bio-Rad; # 4561035) in 1× Tris/Glycine/SDS running buffer (Bio-Rad; #1610732)
44 at a voltage of 125V for 70 min. Proteins were transferred on methanol-activated 0.45 µm
45 Immun-Blot Low Fluorescence polyvinylidene fluoride (PVDF) membranes using the Trans-
46 Blot Turbo RTA Mini 0.45 µm LF PVDF Transfer Kit (Bio-Rad; #1704274). The PVDF

membranes were blocked with 1× VWR Life Science Rapidblock Blocking Solution (VWR; #97064-124) for 1 h at room temperature. Subsequently, the membranes were incubated overnight at +4°C with primary antibody diluted in blocking solution. The membranes were washed four times with TBST (1× Bio-Rad Tris Buffered Saline containing 0.1% Tween-20) and then incubated with secondary antibody, along with hFAB Rhodamine Anti-Actin Primary Antibody (Recombinant human β-actin), diluted in Blocking Solution for 1 h at room temperature, and washed four times with TBST. Fluorescent blots were imaged on the ChemiDoc MP Imaging system using an appropriate detection channel with Image Lab Touch Software (Bio-Rad).

We used antibodies (Abs): Rabbit anti-ZAP IgG Abs (1:1,000 dilution; ANTI-ZC3HAV1; #HPA059096-100UL, Sigma-Aldrich), Rabbit anti-Zika virus NS5 IgG Abs (1:1,000 dilution; #GTX133312, GeneTex), hFAB Rhodamine Anti-Actin Primary Abs (1:2,500; #12004164, Bio-Rad), and IRDye 680RD Goat anti-Rabbit IgG secondary Abs (1:10,000; #926-68071; LI-COR).

Reverse transcriptase quantitative polymerase chain reaction assays (RT-qPCR)

The portion of RNA from all RNA-seq samples described above was used to quantify intracellular Zika virus RNA with a virus-specific RT-qPCR assay. All RT-qPCR reactions were performed on the QuantStudio 3 real-time PCR system (Applied Biosystems) and analyzed using QuantStudio Design & Analysis Software v1.5.2.

For Zika virus RNA quantification, a previously validated SYBR one-step RT-qPCR assay was used [7]. The reaction mixture (20 μL) of the Luna Universal One-Step RT-qPCR Kit (NEB; # E3005L) comprised 10 μL Luna Universal One-Step Reaction Mix, 1 μL Luna WarmStart RT Enzyme Mix, 0.8 μL (10 μM) each of forward (ZIKV-F-SYBR: 5′-

70 AGGATCATAGGTGATGAAGAAAAGT-3′) and reverse (ZIKV-R-SYBR: 5′-
71 CCTGACAACACTAAGATTGGTGC-3′) primers, 3.4 µL nuclease-free water, and 4 µL of
72 RNA template. The reverse transcription and enzyme activation steps of 10 min at 55°C and 1
73 min at 95°C were followed by 40 amplification cycles (10 s at 95°C and 60 s at 60°C). For a
74 standard curve, we generated complementary DNA fragment using viral RNA as a template and
75 primers (T7-F3- TAATACGACTCACTATAGGGCACCACCTGGGCTG; R3-
76 ACAGGCTGCACAGCTTTCCC) containing the T7 promoter. Afterward, the DNA template
77 was transcribed with the MAXIscript™ T7 Transcription Kit (Fisher; #10430355) to generate
78 Zika virus RNA. DNA was removed with the TURBO DNase (Fisher; # AM2238) and was
79 purified with RNA Clean & Concentrator-5 kit (ZYMO; # R1016) following Qubit RNA High
80 Sensitivity Kit (Fisher; # Q32855) quantification. The purified RNA was used to generate the
81 standard curve and quantify Zika RNA loads as we previously described [6,8]. Zika virus RNA
82 copies were expressed per 100 ng of total RNA quantified with the Qubit RNA High Sensitivity
83 Kit. Strict precautions were taken to prevent PCR contamination. All master mix preparations
84 were done in the dedicated PCR cabinet. Aerosol-resistant filter pipette tips and disposable
85 gloves were used. Kit reagent controls were included in every RNA extraction and PCR run.
86

87 **Cytopathic effect kinetics in wild-type and ZAP knockout cells**

88 VERO-ZAP-WT and VERO-ZAP-KO cells were seeded in 6-well plates in DMEM
89 supplemented with 10% FBS. After 24 h, the cell culture medium was removed, and monolayers
90 were gently washed twice with 1× PBS. Cell monolayers were then mock-infected or infected (3
91 replicates) with wild-type Zika virus H/2013/PF at an MOI of 1 in 1 mL of DMEM and plates
92 were incubated at 37 °C for 2 h in a 5% CO_2 incubator. Following the incubation period, the

93 inoculum was removed, and monolayers were washed twice with 1× PBS. Subsequently, 3 mL
94 of DMEM supplemented with 2% FBS was added to each well, and plates were further incubated
95 at 37°C in a 5% CO_2 incubator. Cells were observed under a light microscope for any visible
96 cytopathic effect.
97
98 **Cell viability assay**
99 Wild-type and VERO-ZAP-KO cells were mock-inoculated or Zika virus-inoculated in suspension
100 at an MOI of 1 in 200 µL of DMEM supplemented with 10% FBS. Tubes with inoculated cells
101 were incubated at 37 °C for 1 h and shaken gently every 10 min. Then, cells were washed with cell
102 culture media, and 50 µL of cell suspension was seeded in 96-well plates prefilled with 50 µL of
103 medium. The final seeding concentration was 5×10^4 cells per well. Plates corresponding to
104 different experimental time points were infected at the same initial time. Mock-infected cells and
105 medium-only wells were also included as controls in each plate. The assay was performed in four
106 biological and three technical replicates.
107 At 24 h, 48 h, 72 h, 96 h, and 120 h, cells were analyzed with the CellTiter-Glo Luminescent Assay
108 (Promega; # G7572) according to the manufacturer's instructions. For analysis, 96-well black
109 plates (PerkinElmer) and CellTiter-Glo reagent were equilibrated to room temperature for 15 min.
110 Then, 20 µL of CellTiter-Glo reagent was added to each well with cells, and plates were placed on
111 an orbital shaker at 60 rpm for 12 min. The cells containing CellTiter-Glo reagent were mixed well
112 and were transferred to 96-well black plates. Luminescence was quantified on the Promega
113 GloMax Explorer microplate reader (Promega; # GM3500). At each sampling, luminescence data
114 from virus-inoculated cells were normalized by data from mock-inoculated cells to express relative
115 viability.

116 **SUPPLEMENTAL REFERENCES**

117 1. Chapagain S, Pal Singh P, Le K, et al. Japanese encephalitis virus persists in the human
118 reproductive epithelium and porcine reproductive tissues. PLoS Negl Trop Dis. 2022
119 Jul;16(7):e0010656.
120 2. Sabir AJ, Singh PP, Trus I, et al. Asian Zika virus can acquire generic African-lineage mutations
121 during in utero infection. Emerg Microbes Infect. 2023 Dec;12(2):2263592.
122 3. Darbellay J, Lai K, Babiuk S, et al. Neonatal pigs are susceptible to experimental Zika virus
123 infection. Emerg Microbes Infect. 2017 Feb 15;6(2):e6.
124 4. Darbellay J, Cox B, Lai K, et al. Zika Virus Causes Persistent Infection in Porcine Conceptuses and
125 may Impair Health in Offspring. EBioMedicine. 25:73-86.2017.
126 5. Trus I, Udenze D, Cox B, et al. Subclinical in utero Zika virus infection is associated with
127 interferon alpha sequelae and sex-specific molecular brain pathology in asymptomatic porcine
128 offspring. In: Pierson TC, editor. PLoS Pathogens2019. p. e1008038.
129 6. Trus I, Udenze D, Berube N, et al. CpG-Recoding in Zika Virus Genome Causes Host-Age-
130 Dependent Attenuation of Infection With Protection Against Lethal Heterologous Challenge in
131 Mice. Front Immunol. 2019;10:3077.
132 7. Xu MY, Liu SQ, Deng CL, et al. Detection of Zika virus by SYBR green one-step real-time RT-PCR.
133 Journal of virological methods: J Virol Methods; 2016. p. 93-97.
134 8. Udenze D, Trus I, Berube N, et al. The African strain of Zika virus causes more severe in utero
135 infection than Asian strain in a porcine fetal transmission model. Emerging Microbes &
136 Infections. 2019; 8:1098-1107.2019.

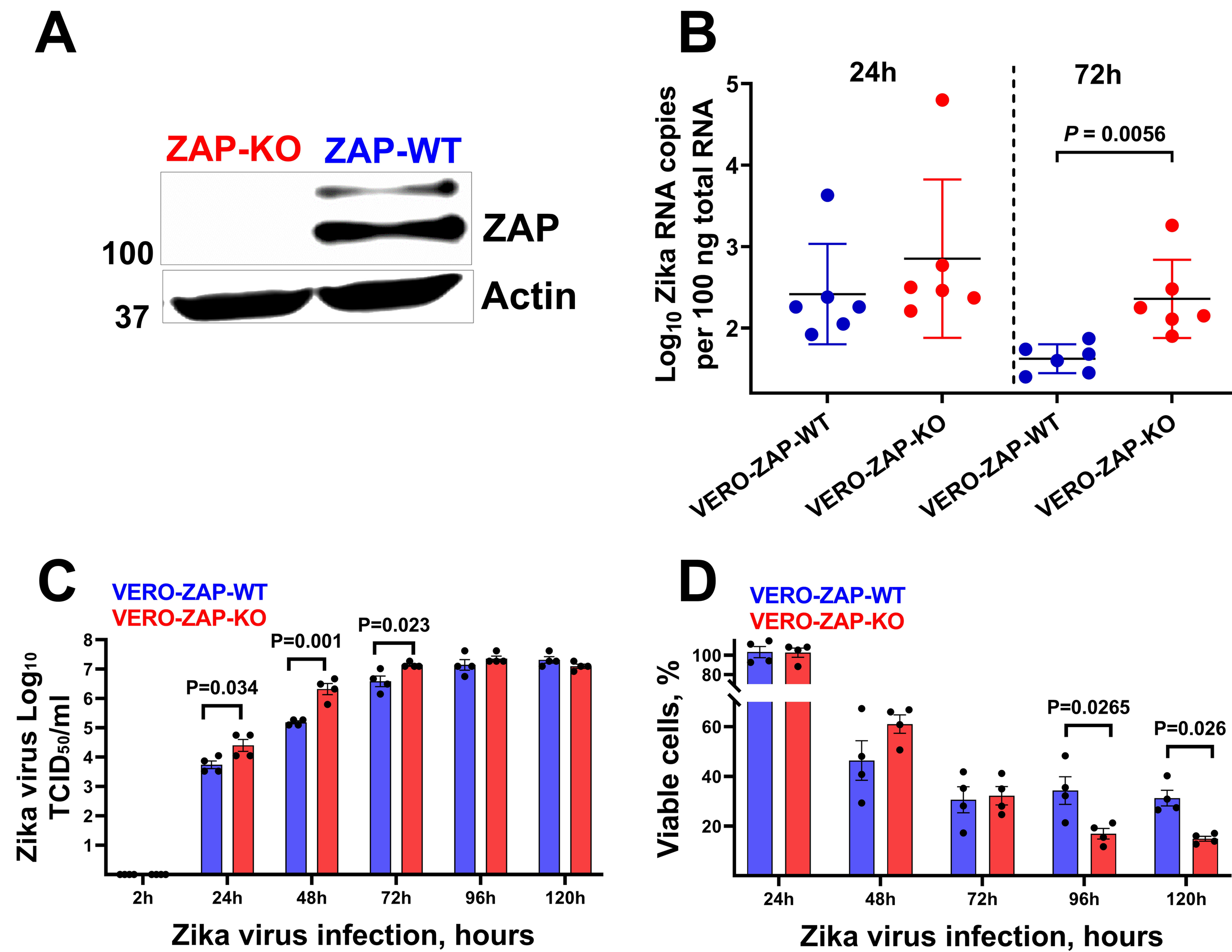
A
ZAP-KO
ZAP-WT
100
37
ZAP
Actin
B
24h
72h
P = 0.0056
Log10 Zika RNA copies per 100 ng total RNA
5
4
3
2
VERO-ZAP-WT
VERO-ZAP-KO
VERO-ZAP-WT
VERO-ZAP-KO
C
VERO-ZAP-WT
VERO-ZAP-KO
P=0.034
P=0.001
P=0.023
Zika virus Log10 TCID50/ml
8
7
6
5
4
3
2
1
2h
24h
48h
72h
96h
120h
Zika virus infection, hours
D
VERO-ZAP-WT
VERO-ZAP-KO
Viable cells, %
100
80
60
40
20
P=0.0265
P=0.026
24h
48h
72h
96h
120h
Zika virus infection, hours

A

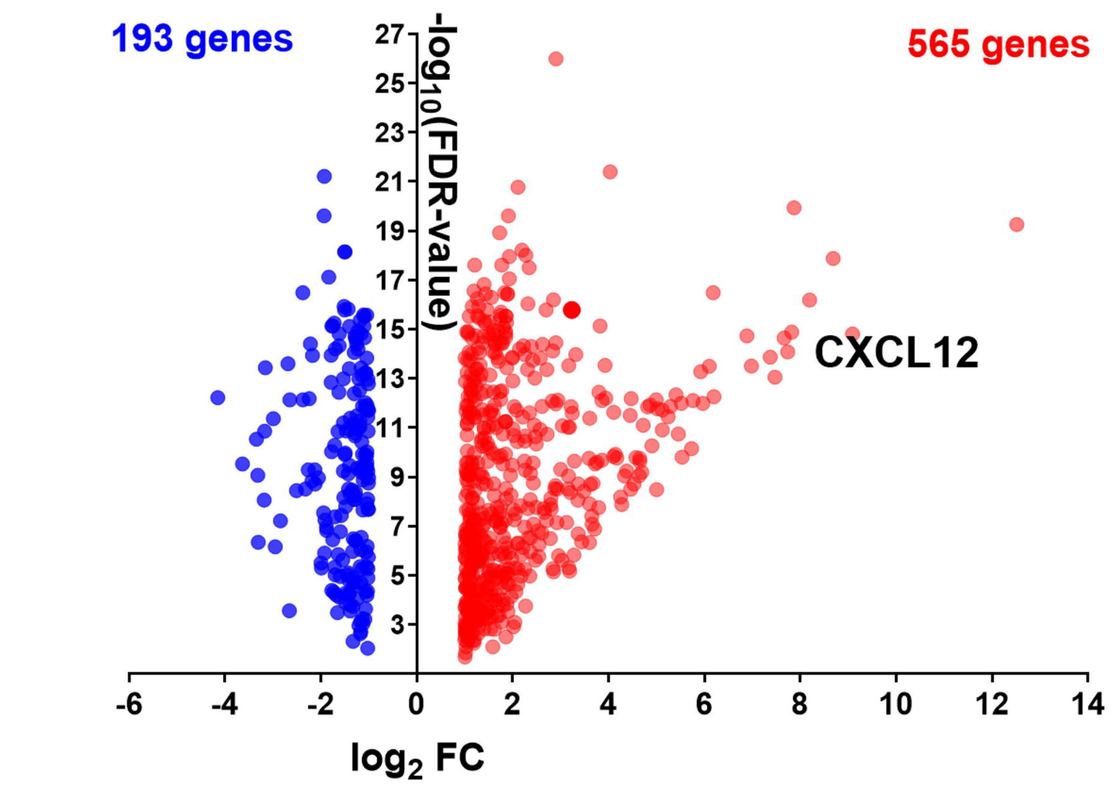
Mock-infected VERO-ZAP-WT vs. VERO-ZAP-KO, 24h
193 genes
565 genes
CXCL12
-log10(FDR-value)
log2 FC

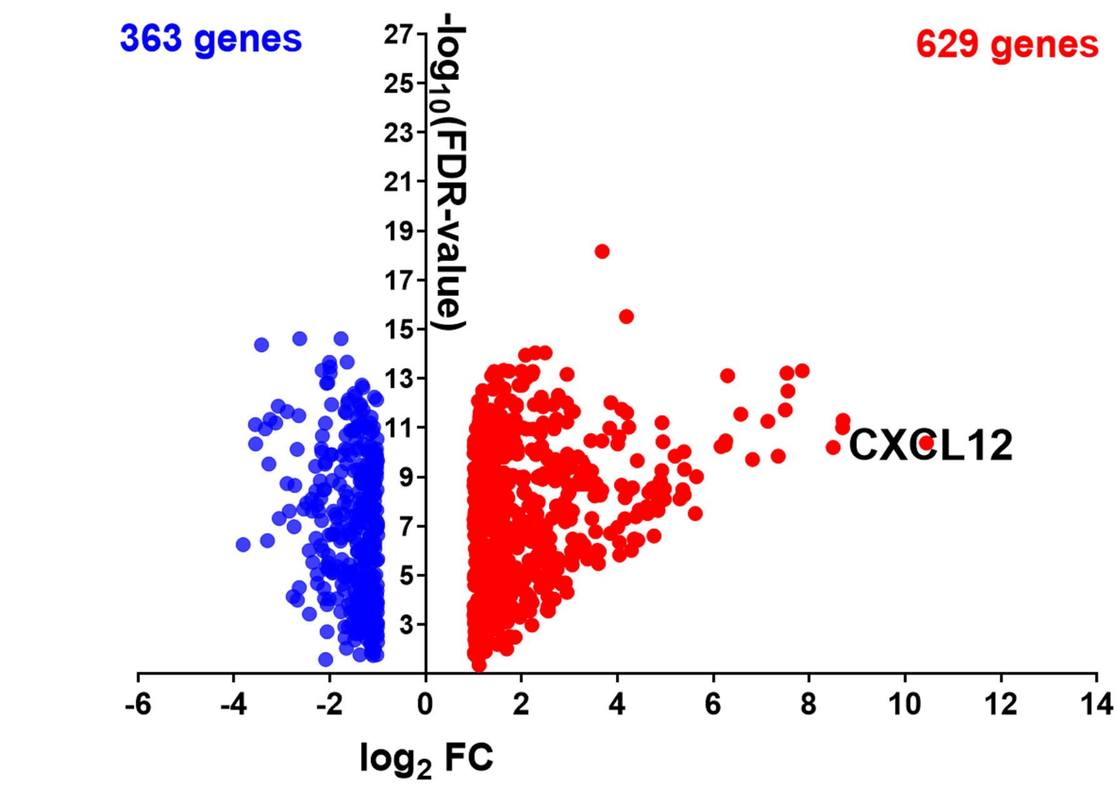
Mock-infected VERO-ZAP-WT vs. VERO-ZAP-KO, 72h
363 genes
629 genes
CXCL12
-log10(FDR-value)
log2 FC

B

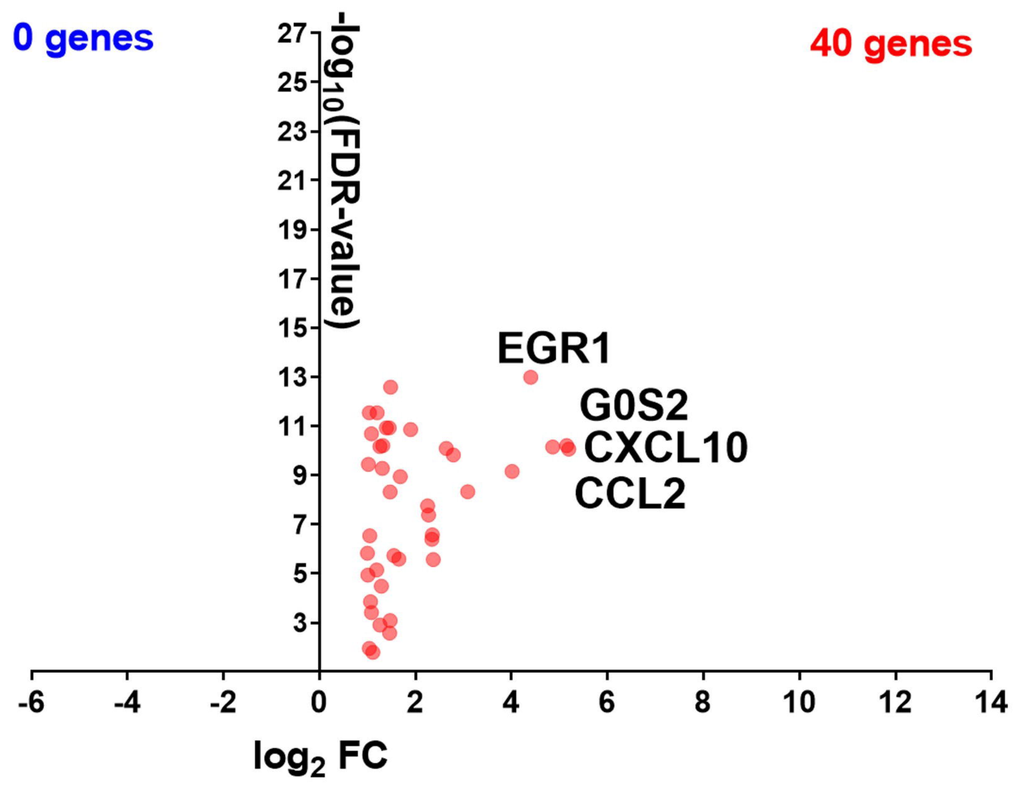
Mock-infected vs. Zika-infected VERO-ZAP-WT, 24h
0 genes
40 genes
EGR1
G0S2
CXCL10
CCL2
-log10(FDR-value)
log2 FC

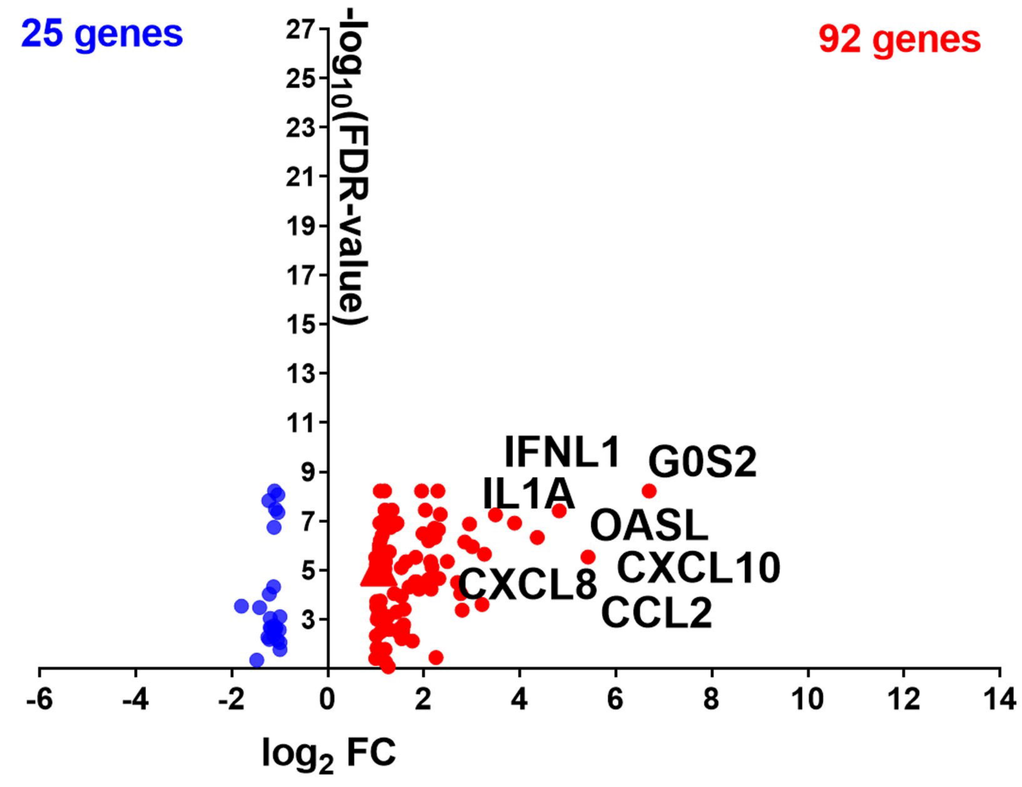
Mock-infected vs. Zika-infected VERO-ZAP-WT, 72h
25 genes
92 genes
IFNL1
G0S2
IL1A
OASL
CXCL10
CXCL8
CCL2
-log10(FDR-value)
log2 FC

C

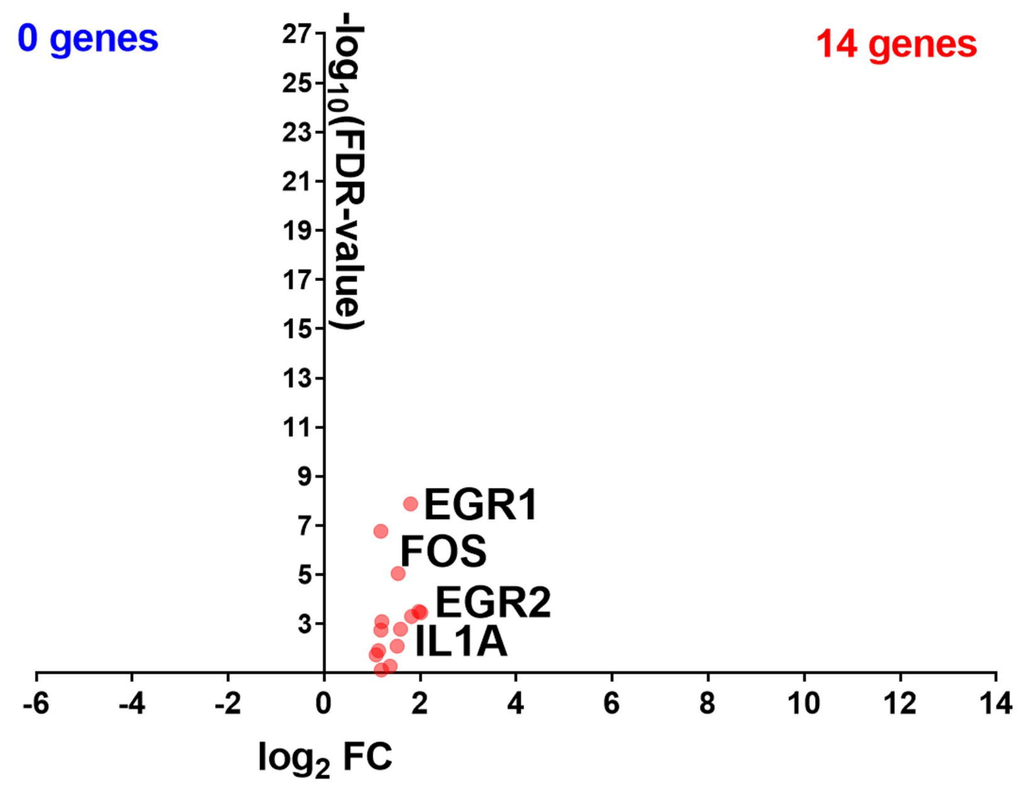
Mock-infected vs. Zika-infected VERO-ZAP-KO, 24h
0 genes
14 genes
EGR1
FOS
EGR2
IL1A
-log10(FDR-value)
log2 FC

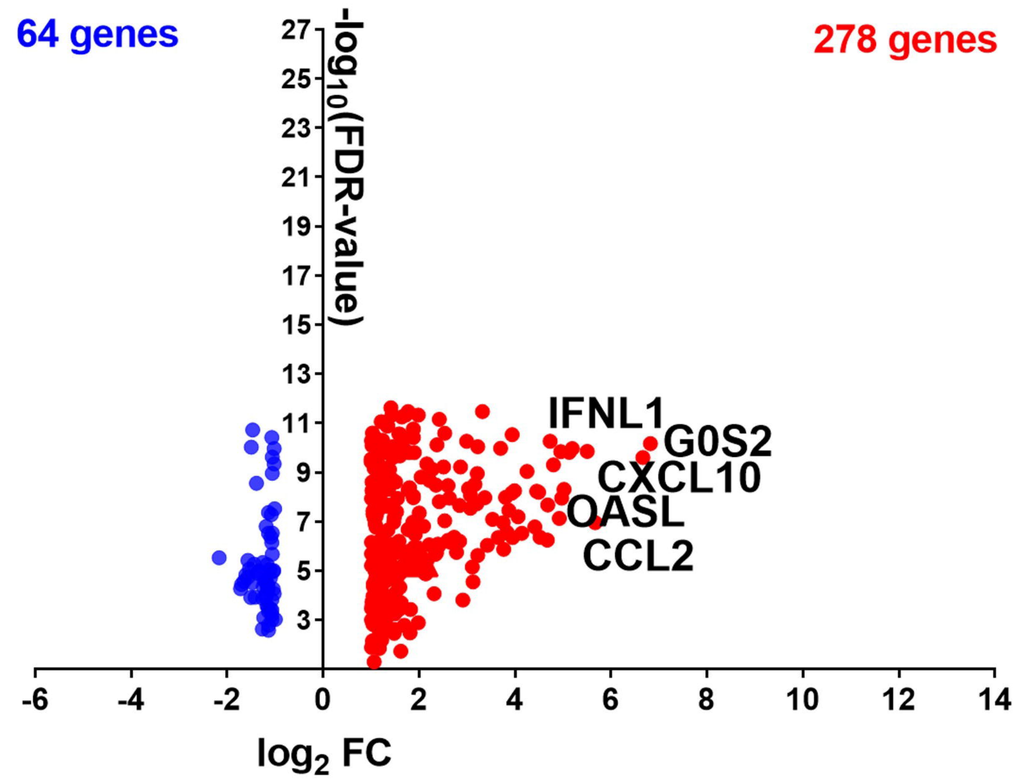
Mock-infected vs. Zika-infected VERO-ZAP-KO, 72h
64 genes
278 genes
IFNL1
G0S2
CXCL10
OASL
CCL2
-log10(FDR-value)
log2 FC

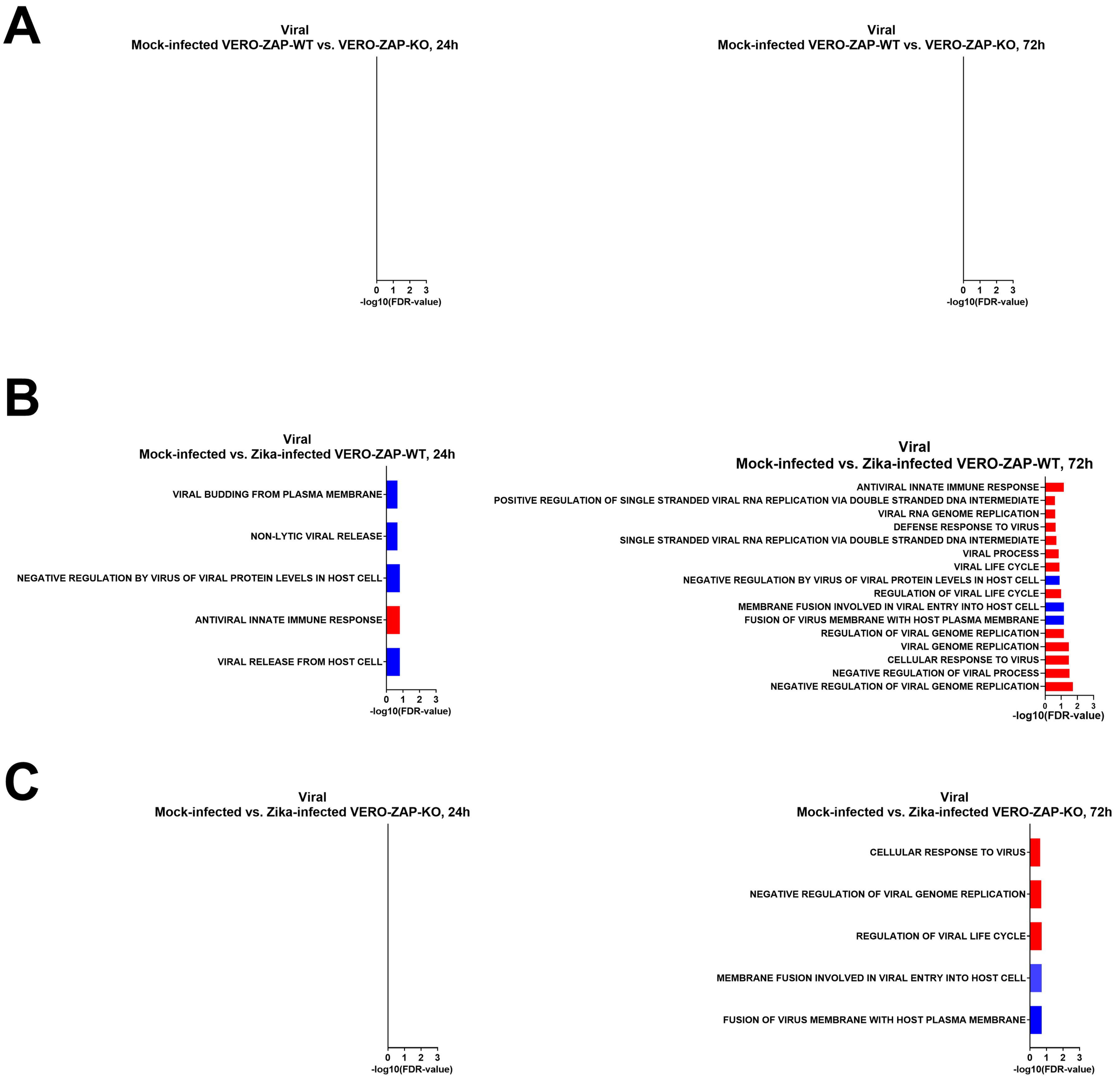
A
Viral
Mock-infected VERO-ZAP-WT vs. VERO-ZAP-KO, 24h
0 1 2 3
-log10(FDR-value)
Viral
Mock-infected VERO-ZAP-WT vs. VERO-ZAP-KO, 72h
0 1 2 3
-log10(FDR-value)
B
Viral
Mock-infected vs. Zika-infected VERO-ZAP-WT, 24h
VIRAL BUDDING FROM PLASMA MEMBRANE
NON-LYTIC VIRAL RELEASE
NEGATIVE REGULATION BY VIRUS OF VIRAL PROTEIN LEVELS IN HOST CELL
ANTIVIRAL INNATE IMMUNE RESPONSE
VIRAL RELEASE FROM HOST CELL
0 1 2 3
-log10(FDR-value)
Viral
Mock-infected vs. Zika-infected VERO-ZAP-WT, 72h
ANTIVIRAL INNATE IMMUNE RESPONSE
POSITIVE REGULATION OF SINGLE STRANDED VIRAL RNA REPLICATION VIA DOUBLE STRANDED DNA INTERMEDIATE
VIRAL RNA GENOME REPLICATION
DEFENSE RESPONSE TO VIRUS
SINGLE STRANDED VIRAL RNA REPLICATION VIA DOUBLE STRANDED DNA INTERMEDIATE
VIRAL PROCESS
VIRAL LIFE CYCLE
NEGATIVE REGULATION BY VIRUS OF VIRAL PROTEIN LEVELS IN HOST CELL
REGULATION OF VIRAL LIFE CYCLE
MEMBRANE FUSION INVOLVED IN VIRAL ENTRY INTO HOST CELL
FUSION OF VIRUS MEMBRANE WITH HOST PLASMA MEMBRANE
REGULATION OF VIRAL GENOME REPLICATION
VIRAL GENOME REPLICATION
CELLULAR RESPONSE TO VIRUS
NEGATIVE REGULATION OF VIRAL PROCESS
NEGATIVE REGULATION OF VIRAL GENOME REPLICATION
0 1 2 3
-log10(FDR-value)
C
Viral
Mock-infected vs. Zika-infected VERO-ZAP-KO, 24h
0 1 2 3
-log10(FDR-value)
Viral
Mock-infected vs. Zika-infected VERO-ZAP-KO, 72h
CELLULAR RESPONSE TO VIRUS
NEGATIVE REGULATION OF VIRAL GENOME REPLICATION
REGULATION OF VIRAL LIFE CYCLE
MEMBRANE FUSION INVOLVED IN VIRAL ENTRY INTO HOST CELL
FUSION OF VIRUS MEMBRANE WITH HOST PLASMA MEMBRANE
0 1 2 3
-log10(FDR-value)

A

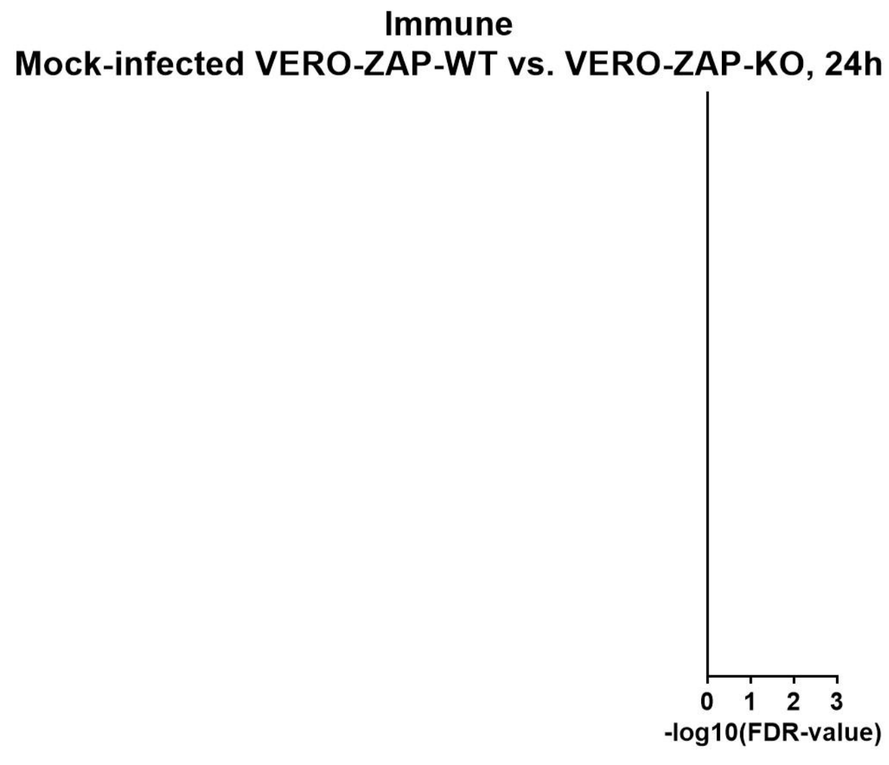
Immune
Mock-infected VERO-ZAP-WT vs. VERO-ZAP-KO, 24h
0 1 2 3
-log10(FDR-value)

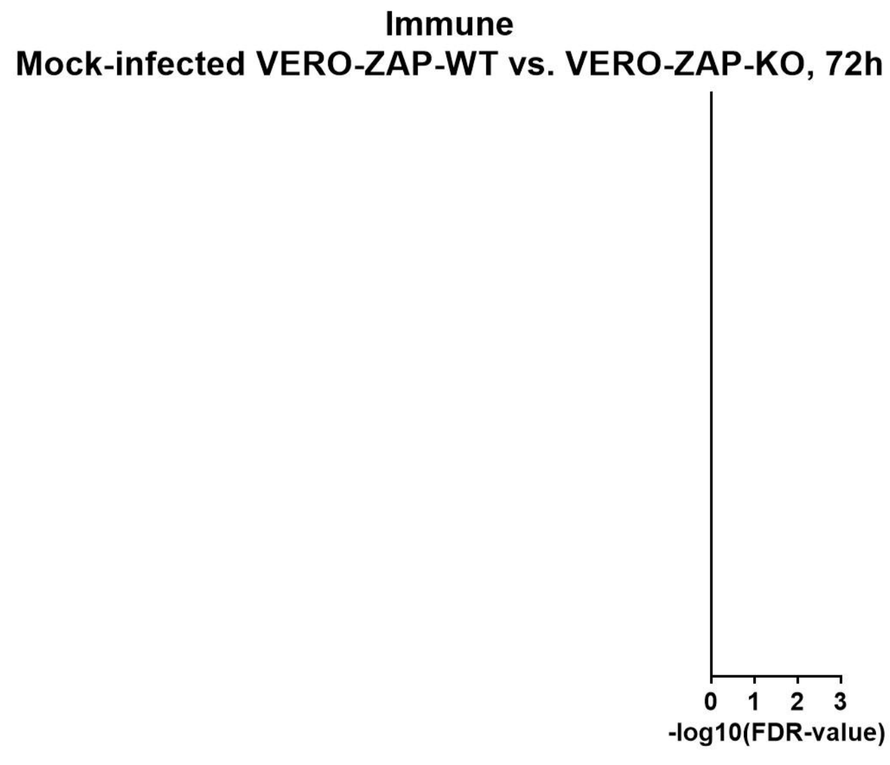
Immune
Mock-infected VERO-ZAP-WT vs. VERO-ZAP-KO, 72h
0 1 2 3
-log10(FDR-value)

B

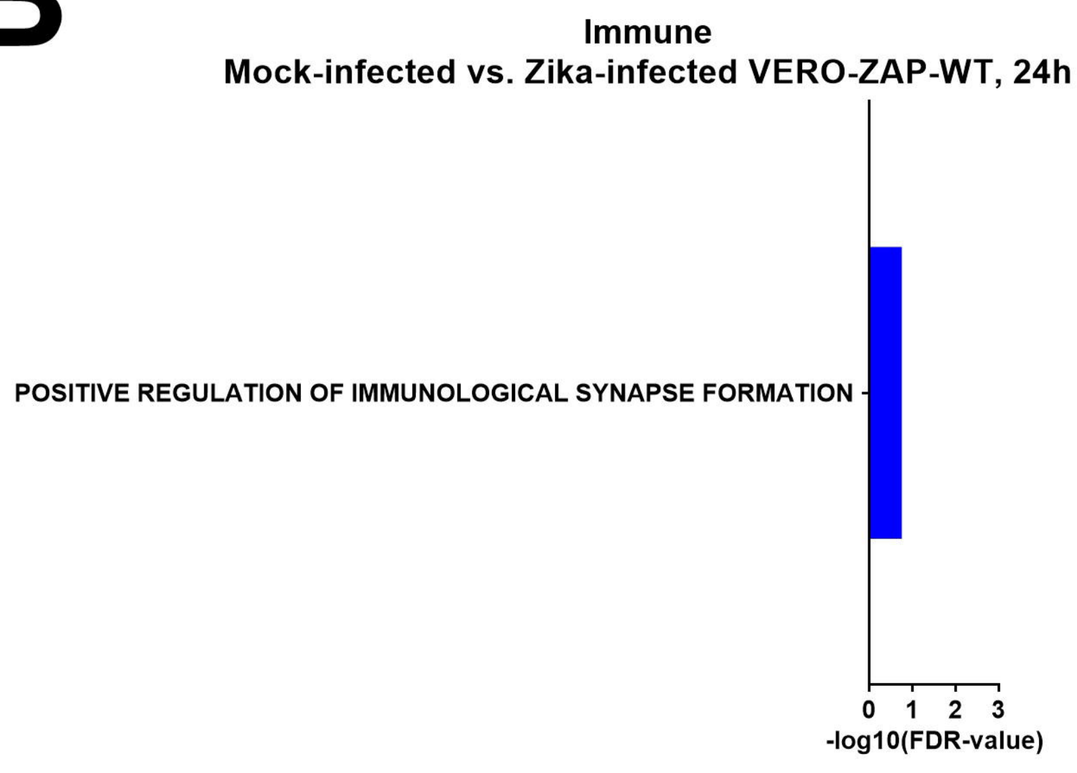
Immune
Mock-infected vs. Zika-infected VERO-ZAP-WT, 24h
POSITIVE REGULATION OF IMMUNOLOGICAL SYNAPSE FORMATION
0 1 2 3
-log10(FDR-value)

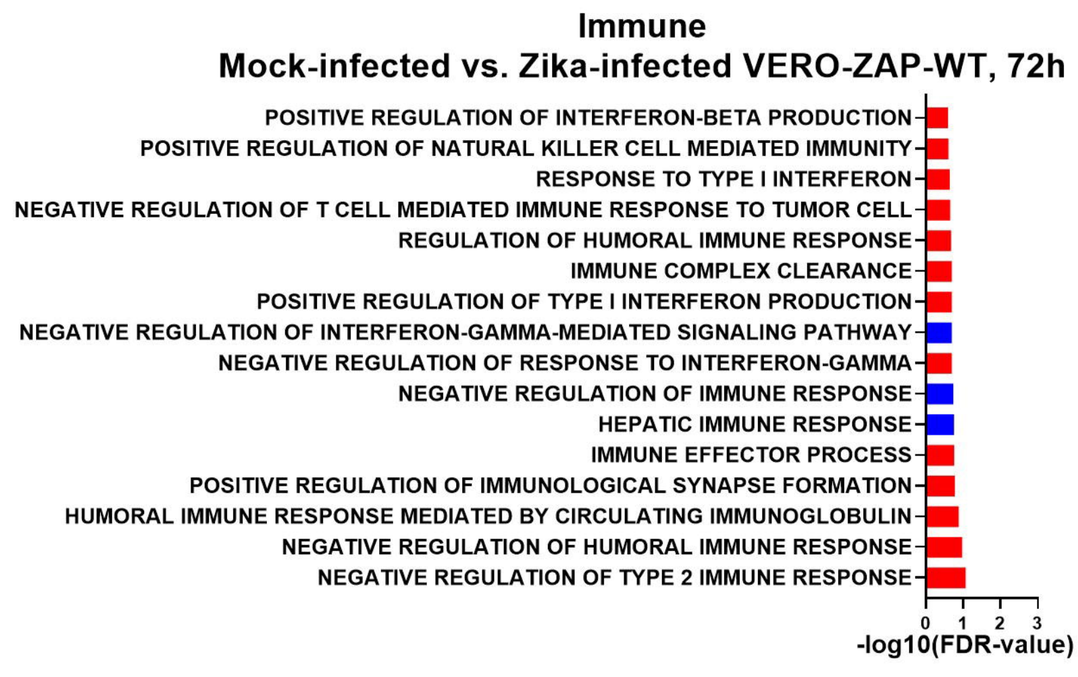
Immune
Mock-infected vs. Zika-infected VERO-ZAP-WT, 72h
POSITIVE REGULATION OF INTERFERON-BETA PRODUCTION
POSITIVE REGULATION OF NATURAL KILLER CELL MEDIATED IMMUNITY
RESPONSE TO TYPE I INTERFERON
NEGATIVE REGULATION OF T CELL MEDIATED IMMUNE RESPONSE TO TUMOR CELL
REGULATION OF HUMORAL IMMUNE RESPONSE
IMMUNE COMPLEX CLEARANCE
POSITIVE REGULATION OF TYPE I INTERFERON PRODUCTION
NEGATIVE REGULATION OF INTERFERON-GAMMA-MEDIATED SIGNALING PATHWAY
NEGATIVE REGULATION OF RESPONSE TO INTERFERON-GAMMA
NEGATIVE REGULATION OF IMMUNE RESPONSE
HEPATIC IMMUNE RESPONSE
IMMUNE EFFECTOR PROCESS
POSITIVE REGULATION OF IMMUNOLOGICAL SYNAPSE FORMATION
HUMORAL IMMUNE RESPONSE MEDIATED BY CIRCULATING IMMUNOGLOBULIN
NEGATIVE REGULATION OF HUMORAL IMMUNE RESPONSE
NEGATIVE REGULATION OF TYPE 2 IMMUNE RESPONSE
0 1 2 3
-log10(FDR-value)

C

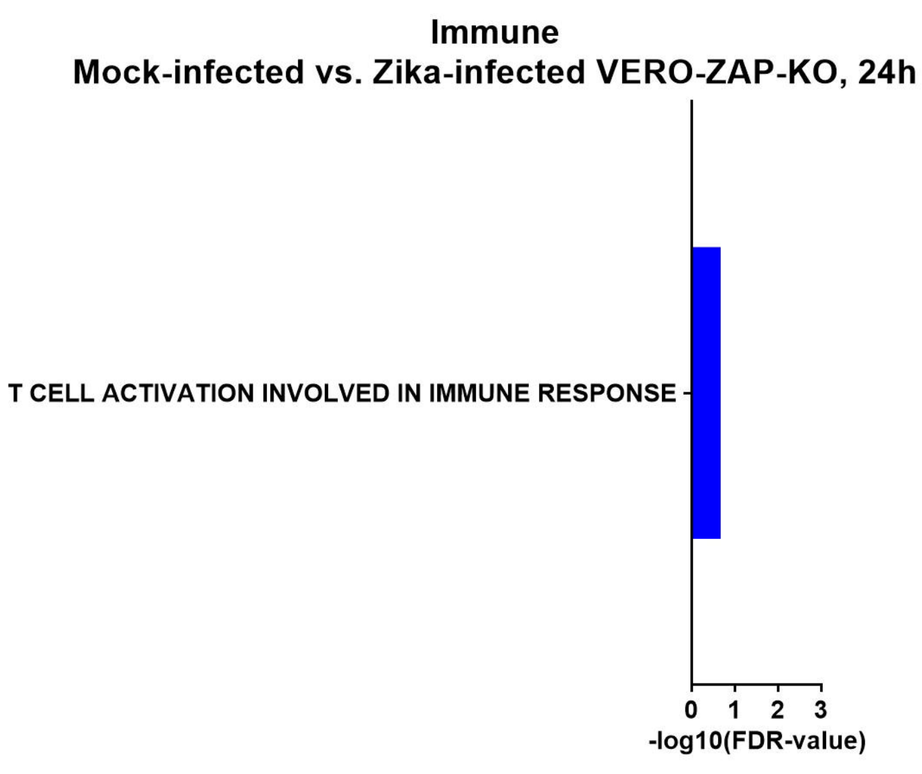
Immune
Mock-infected vs. Zika-infected VERO-ZAP-KO, 24h
T CELL ACTIVATION INVOLVED IN IMMUNE RESPONSE
0 1 2 3
-log10(FDR-value)

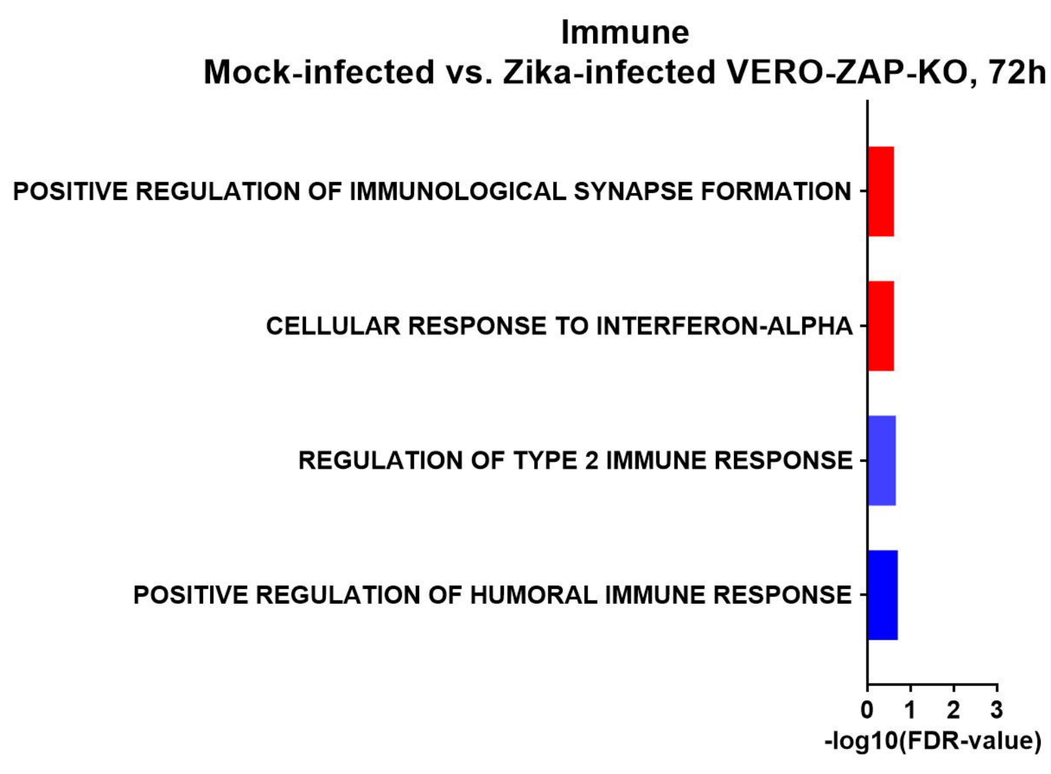
Immune
Mock-infected vs. Zika-infected VERO-ZAP-KO, 72h
POSITIVE REGULATION OF IMMUNOLOGICAL SYNAPSE FORMATION
CELLULAR RESPONSE TO INTERFERON-ALPHA
REGULATION OF TYPE 2 IMMUNE RESPONSE
POSITIVE REGULATION OF HUMORAL IMMUNE RESPONSE
0 1 2 3
-log10(FDR-value)

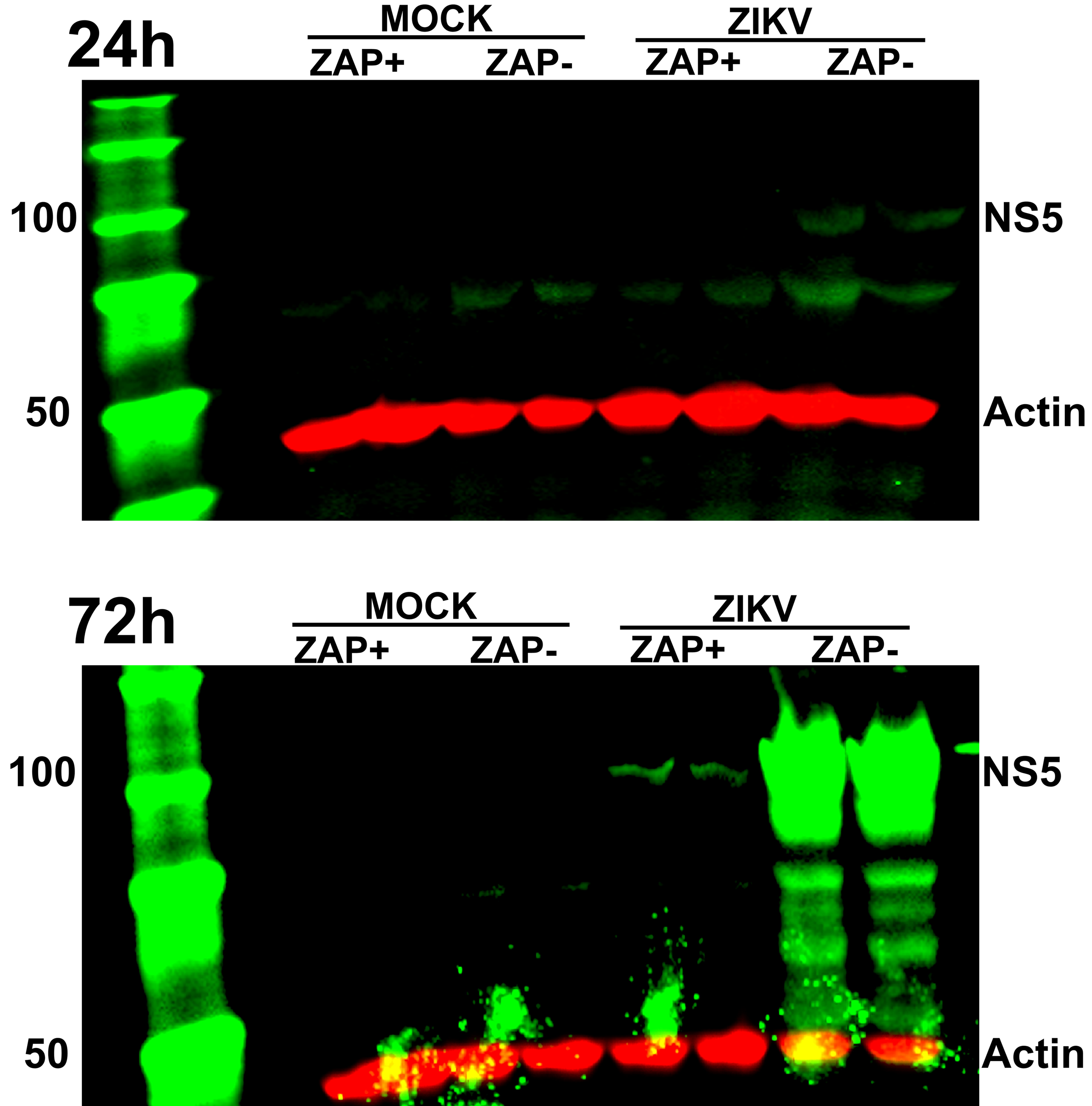
24h
MOCK
ZIKV
ZAP+
ZAP-
ZAP+
ZAP-
100
50
NS5
Actin
72h
MOCK
ZIKV
ZAP+
ZAP-
ZAP+
ZAP-
100
50
NS5
Actin

A

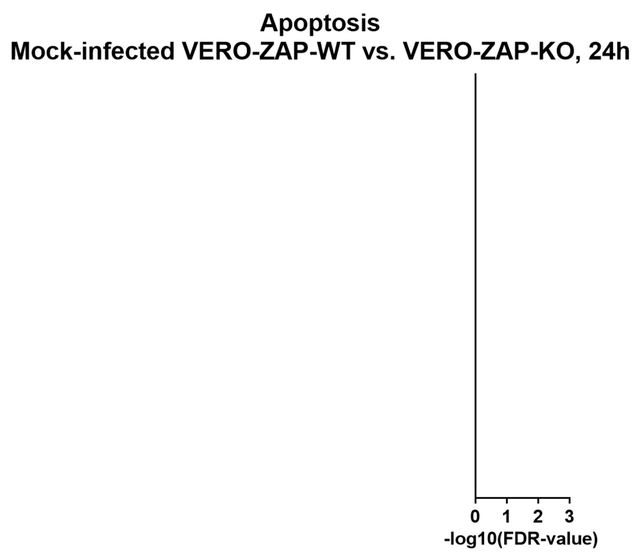
Apoptosis
Mock-infected VERO-ZAP-WT vs. VERO-ZAP-KO, 24h
0 1 2 3
-log10(FDR-value)

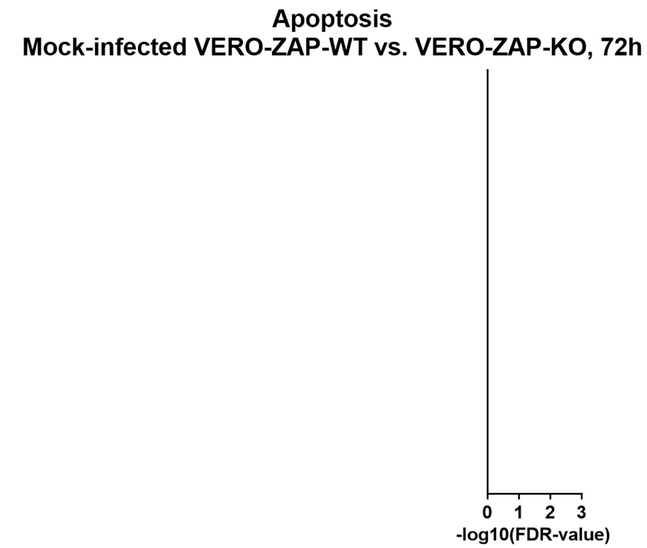
Apoptosis
Mock-infected VERO-ZAP-WT vs. VERO-ZAP-KO, 72h
0 1 2 3
-log10(FDR-value)

B

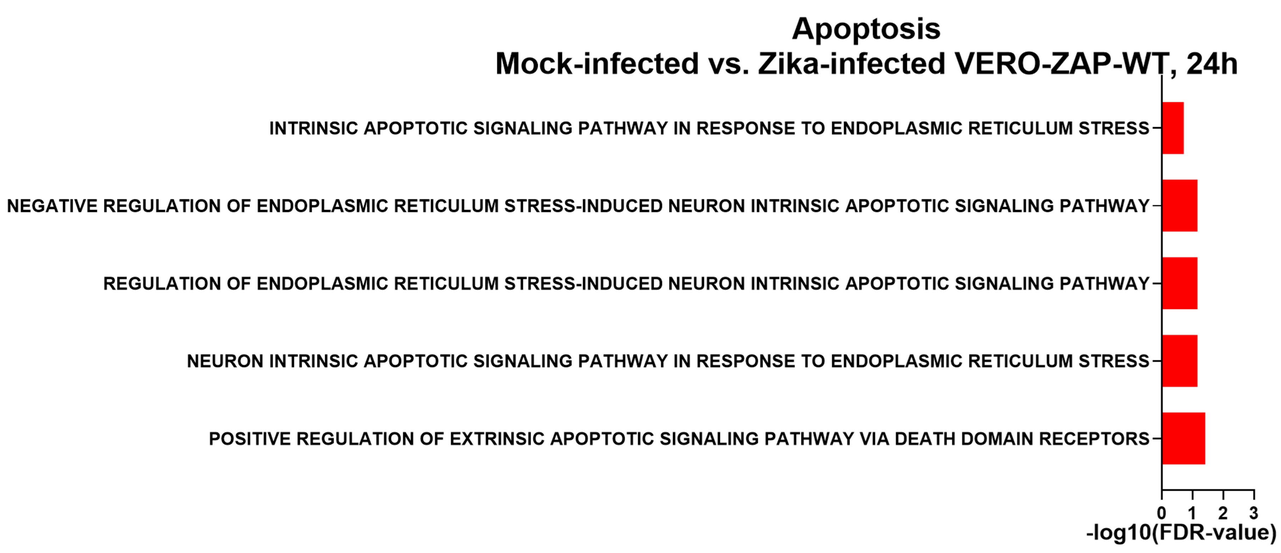
Apoptosis
Mock-infected vs. Zika-infected VERO-ZAP-WT, 24h
INTRINSIC APOPTOTIC SIGNALING PATHWAY IN RESPONSE TO ENDOPLASMIC RETICULUM STRESS
NEGATIVE REGULATION OF ENDOPLASMIC RETICULUM STRESS-INDUCED NEURON INTRINSIC APOPTOTIC SIGNALING PATHWAY
REGULATION OF ENDOPLASMIC RETICULUM STRESS-INDUCED NEURON INTRINSIC APOPTOTIC SIGNALING PATHWAY
NEURON INTRINSIC APOPTOTIC SIGNALING PATHWAY IN RESPONSE TO ENDOPLASMIC RETICULUM STRESS
POSITIVE REGULATION OF EXTRINSIC APOPTOTIC SIGNALING PATHWAY VIA DEATH DOMAIN RECEPTORS
0 1 2 3
-log10(FDR-value)

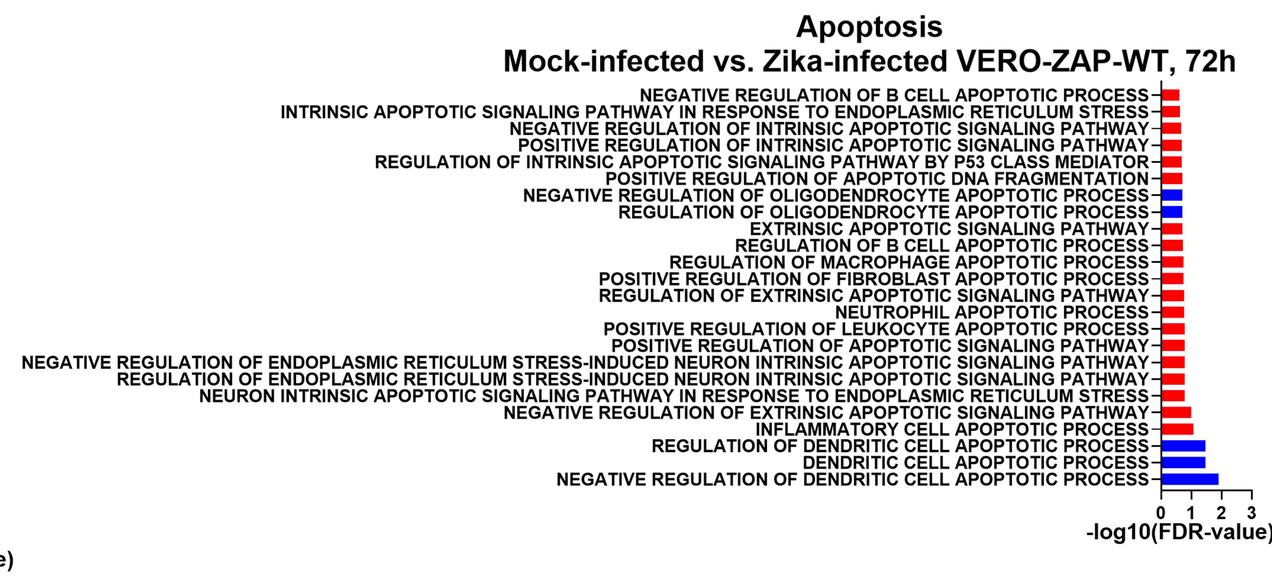
Apoptosis
Mock-infected vs. Zika-infected VERO-ZAP-WT, 72h
NEGATIVE REGULATION OF B CELL APOPTOTIC PROCESS
INTRINSIC APOPTOTIC SIGNALING PATHWAY IN RESPONSE TO ENDOPLASMIC RETICULUM STRESS
NEGATIVE REGULATION OF INTRINSIC APOPTOTIC SIGNALING PATHWAY
POSITIVE REGULATION OF INTRINSIC APOPTOTIC SIGNALING PATHWAY
REGULATION OF INTRINSIC APOPTOTIC SIGNALING PATHWAY BY P53 CLASS MEDIATOR
POSITIVE REGULATION OF APOPTOTIC DNA FRAGMENTATION
NEGATIVE REGULATION OF OLIGODENDROCYTE APOPTOTIC PROCESS
REGULATION OF OLIGODENDROCYTE APOPTOTIC PROCESS
EXTRINSIC APOPTOTIC SIGNALING PATHWAY
REGULATION OF B CELL APOPTOTIC PROCESS
REGULATION OF MACROPHAGE APOPTOTIC PROCESS
POSITIVE REGULATION OF FIBROBLAST APOPTOTIC PROCESS
REGULATION OF EXTRINSIC APOPTOTIC SIGNALING PATHWAY
NEUTROPHIL APOPTOTIC PROCESS
POSITIVE REGULATION OF LEUKOCYTE APOPTOTIC PROCESS
POSITIVE REGULATION OF APOPTOTIC SIGNALING PATHWAY
NEGATIVE REGULATION OF ENDOPLASMIC RETICULUM STRESS-INDUCED NEURON INTRINSIC APOPTOTIC SIGNALING PATHWAY
REGULATION OF ENDOPLASMIC RETICULUM STRESS-INDUCED NEURON INTRINSIC APOPTOTIC SIGNALING PATHWAY
NEURON INTRINSIC APOPTOTIC SIGNALING PATHWAY IN RESPONSE TO ENDOPLASMIC RETICULUM STRESS
NEGATIVE REGULATION OF EXTRINSIC APOPTOTIC SIGNALING PATHWAY
INFLAMMATORY CELL APOPTOTIC PROCESS
REGULATION OF DENDRITIC CELL APOPTOTIC PROCESS
DENDRITIC CELL APOPTOTIC PROCESS
NEGATIVE REGULATION OF DENDRITIC CELL APOPTOTIC PROCESS
0 1 2 3
-log10(FDR-value)

C

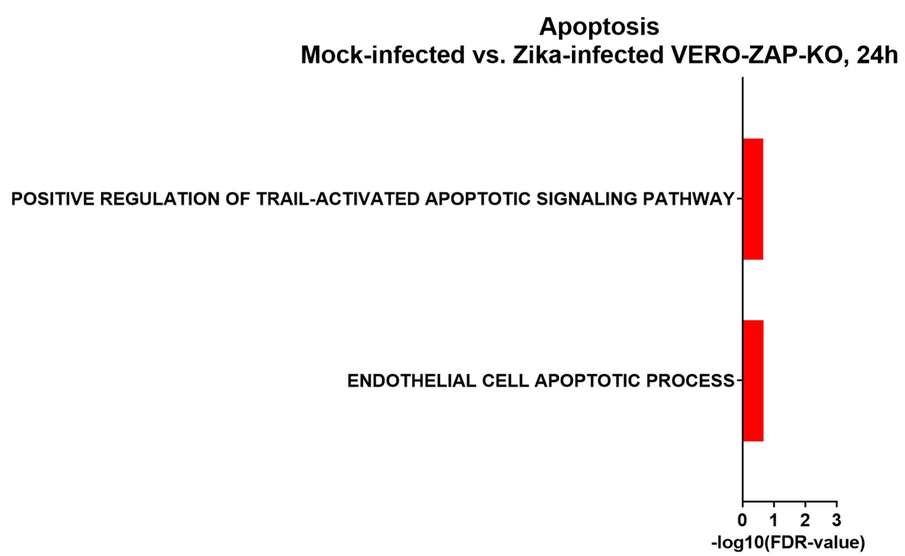
Apoptosis
Mock-infected vs. Zika-infected VERO-ZAP-KO, 24h
POSITIVE REGULATION OF TRAIL-ACTIVATED APOPTOTIC SIGNALING PATHWAY
ENDOTHELIAL CELL APOPTOTIC PROCESS
0 1 2 3
-log10(FDR-value)

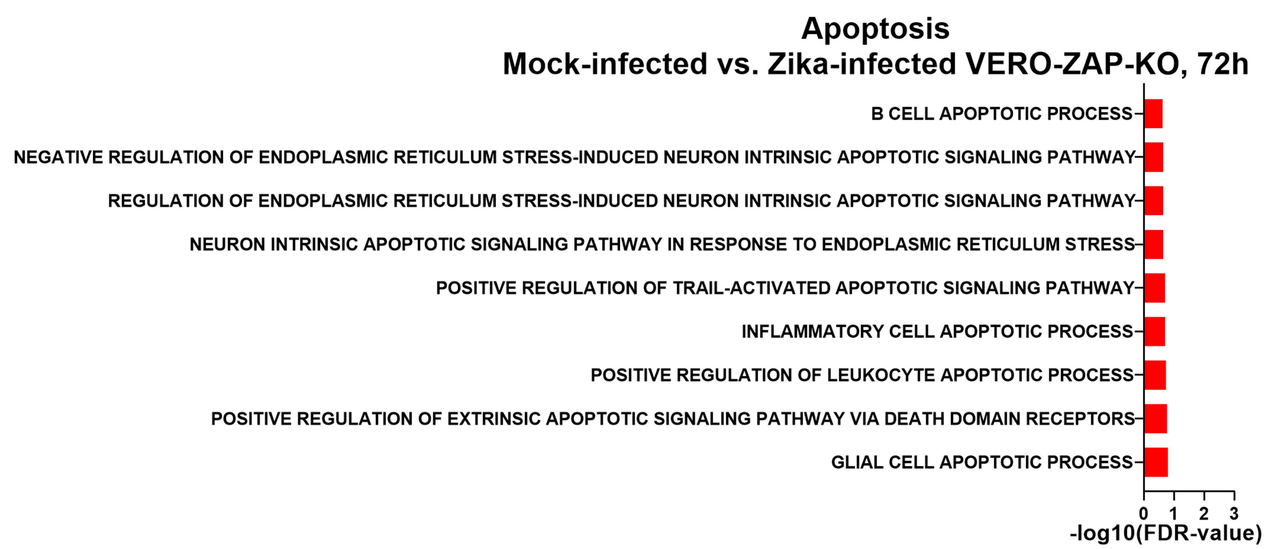
Apoptosis
Mock-infected vs. Zika-infected VERO-ZAP-KO, 72h
B CELL APOPTOTIC PROCESS
NEGATIVE REGULATION OF ENDOPLASMIC RETICULUM STRESS-INDUCED NEURON INTRINSIC APOPTOTIC SIGNALING PATHWAY
REGULATION OF ENDOPLASMIC RETICULUM STRESS-INDUCED NEURON INTRINSIC APOPTOTIC SIGNALING PATHWAY
NEURON INTRINSIC APOPTOTIC SIGNALING PATHWAY IN RESPONSE TO ENDOPLASMIC RETICULUM STRESS
POSITIVE REGULATION OF TRAIL-ACTIVATED APOPTOTIC SIGNALING PATHWAY
INFLAMMATORY CELL APOPTOTIC PROCESS
POSITIVE REGULATION OF LEUKOCYTE APOPTOTIC PROCESS
POSITIVE REGULATION OF EXTRINSIC APOPTOTIC SIGNALING PATHWAY VIA DEATH DOMAIN RECEPTORS
GLIAL CELL APOPTOTIC PROCESS
0 1 2 3
-log10(FDR-value)

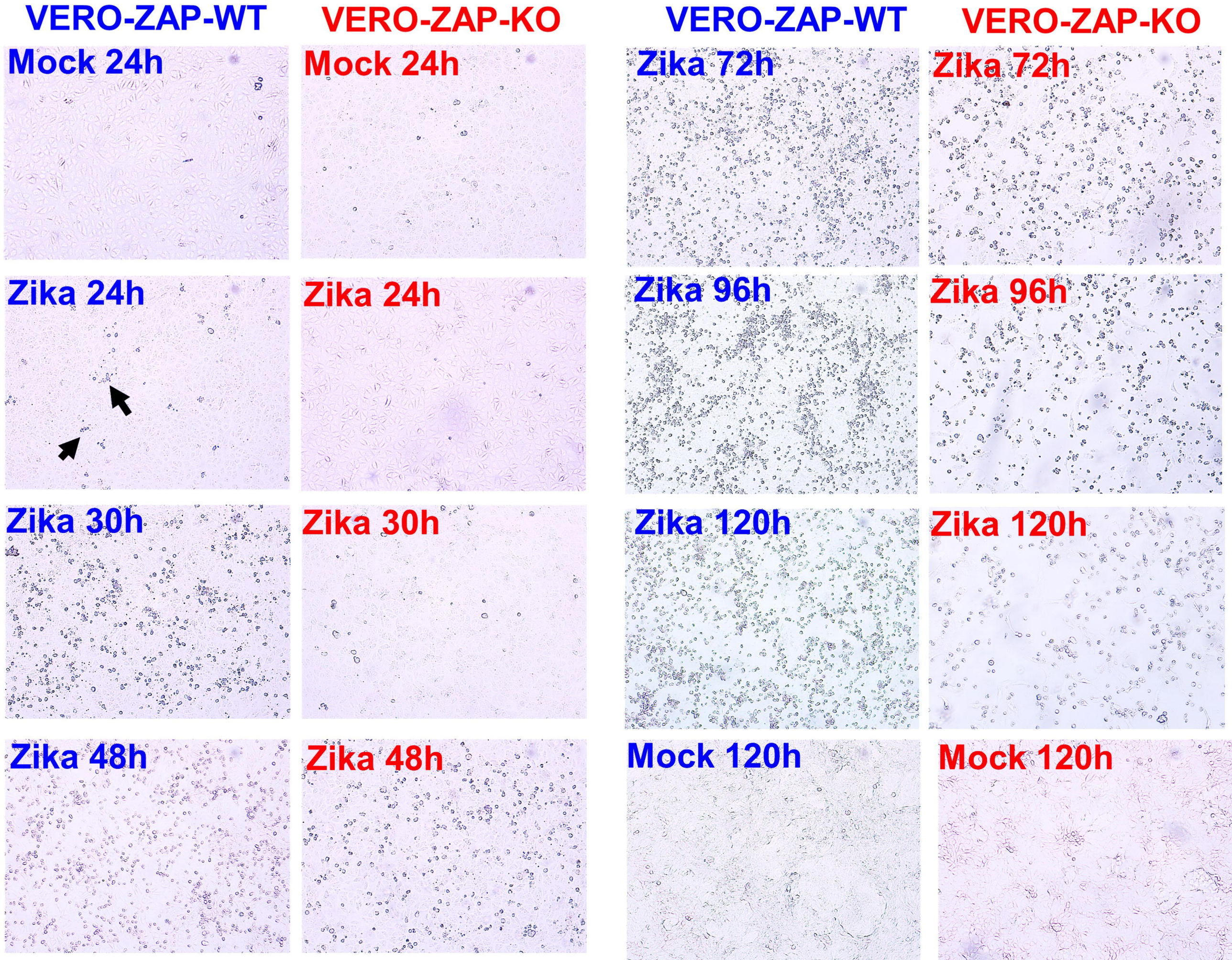
VERO-ZAP-WT
VERO-ZAP-KO
VERO-ZAP-WT
VERO-ZAP-KO
Mock 24h
Mock 24h
Zika 72h
Zika 72h
Zika 24h
Zika 24h
Zika 96h
Zika 96h
Zika 30h
Zika 30h
Zika 120h
Zika 120h
Zika 48h
Zika 48h
Mock 120h
Mock 120h